Quaternary Science Reviews 286 (2022) 107527

Contents lists available at ScienceDirect

Quaternary Science Reviews

journal homepage: www.elsevier.com/locate/quascirev

An exceptional record of millennial-scale climate variability in the southern Iberian Margin during MIS 6: Impact on the formation of sapropel S6

Francisco J. Sierro [a, *], Nils Andersen [b]

[a] Dept. de Geología, Univ. de Salamanca, Plaza de los Caídos s/n, 37008, Salamanca, Spain
[b] Leibniz-Laboratory for Radiometric Dating and Isotope Research, Christian-Albrechts-Universität zu Kiel, Kiel, Germany

ARTICLE INFO

Article history:
Received 30 July 2021
Received in revised form
4 April 2022
Accepted 19 April 2022
Available online 11 May 2022

Handling Editor: Dr A. Voelker

Keywords:
Mediterranean overflow
MIS6
Penultimate glaciation
Millennial climate change
Sapropel
Mediterranean overturning
Meltwater
Ice sheets

ABSTRACT

The study of planktic and benthic $\delta^{18}O$ at site U1389 in the Gulf of Cadiz allowed us to reconstruct climate variability during the penultimate glacial period at an unprecedented millennial scale resolution. Hereby, a sequence of interstadial-stadial episodes similar to the Dansgaard-Oeschger events recorded during Marine Isotope Stage (MIS)3, were recognized in MIS6. After a detailed correlation with millennial-scale variability recorded along the Iberian margin and the North Atlantic we were able to link the millennial changes next to the Iberian Peninsula with Antarctic climate variability due to the interhemispheric seesaw response of the Atlantic circulation. The straight coupling at site U1389 of a) the planktic $\delta^{18}O$ that reflects climate change in the Atlantic with b) the benthic $\delta^{18}O$, which records the temperature and oxygen isotope composition of the mixture of Mediterranean Outflow and Atlantic intermediate water, indicates that millennial climate variability also had a strong impact on the eastern Mediterranean. The detailed analysis of the benthic $\delta^{13}C$ and the fine sand content in the sediments from site U1389 led us to recognize the response of the Mediterranean overflow water (MOW) to millennial scale changes in Mediterranean overturning circulation during the penultimate glaciation. Both Mediterranean Overturning Circulation and MOW strength increased at times of cool and arid climates and weakened during warm and more humid episodes, similar to what has been described for MIS3. The tuning of MOW weakening events occurring at times of precession minima with eastern Mediterranean sapropels and enhanced Asian monsoon allowed the elaboration of a new chronology for MIS6. It was compared with the Epica Dome C time scale, which was also based on the tuning of atmospheric $\delta^{18}O$ with Asian Monsoons speleothem records.

Mediterranean overturning during MIS6 was also strongly affected by freshwater perturbations occurring at times of insolation maxima, leading to the formation of the “glacial sapropel” S6. Two major drops in seawater $\delta^{18}O$ centered at 175 and 150 ky were observed near the entrance of the Mediterranean that were related to meltwater released from the ice sheets, coinciding with periods of insolation maxima. The entry of this meltwater anomaly through the Strait of Gibraltar is clearly registered in the western and eastern Mediterranean, especially at the onset of sapropel S6, suggesting that it was a major component of the freshwater that initiated the buoyancy gain preceding deep water stagnation.

1. Introduction

Greenland ice cores have shown a millennial-scale, highly resolved climate record for the last glacial period and similar, high-resolution records, have been obtained in deep sea sediment cores. Some of the most reliable records have been obtained in the Iberian Margin since the seminal work of Shackleton et al. (2000). The climate records from this region have been a laboratory to investigate the interhemispheric seesaw millennial climate change during the last glacial period (de Abreu et al., 2003; Goni et al., 2000; Hodell et al., 2013a; Margari et al., 2010; Martrat et al., 2007; Skinner et al., 2003; Skinner and Elderfield, 2007; Voelker and de Abreu, 2011). Numerous works have revealed the straight coupling between sea surface temperature (SST) and surface

* Corresponding author.
E-mail address: sierro@usal.es (F.J. Sierro).

https://doi.org/10.1016/j.quascirev.2022.107527

oxygen isotope records in the NE Atlantic and climate records in Greenland ice cores, while deep water properties changed in phase with Antarctic climate (Hodell et al., 2013a; Shackleton et al., 2000). Northward heat transport in the Atlantic warms the high latitudes of the northern Hemisphere and cool the Antarctic (Broecker, 1998; Stocker, 1998).

However, Greenland ice core records only extend back to 124 ky because the ice accumulated during the penultimate glacial period is not adequate for paleoclimate studies (Chappellaz et al., 1997). Pollen and stable isotope records in core MD01-2444 from the Iberian margin registered abrupt climate change during the penultimate glacial period (Hodell et al., 2013a; Margari et al., 2010; Martrat et al., 2007). Although the stable oxygen isotope record in core MD01-2444 was elaborated at the maximum allowed resolution, some details of the centennial-millennial Dansgaard-Oeschger type events for MIS6 are not visible. Although there are some marine climate records for MIS6 in the Mediterranean region (Cortina et al., 2011; Martrat et al., 2004) complemented with a few studies of speleothem and pollen archives on land (Ayalon et al., 2002; Nehme et al., 2018; Regattieri et al., 2021a; Roucoux et al., 2011; Wainer et al., 2013; Wilson et al., 2021), millennial-scale climate variability during the penultimate glacial period is not well known.

In this study, the exceptional high sedimentation rates at site U1389 allowed to obtain a higher-resolution stable isotope record for MIS6 that can provide a more detailed record of millennial-scale climate events during the penultimate glacial period and can be used as a reference record for millennial-scale climate variability in the north Atlantic. Because of the proximity of this site to the Strait of Gibraltar and the influence of the Mediterranean Overflow Water (MOW) in bottom waters at site U1389 the study of the benthic $\delta^{18}O$ and $\delta^{13}C$, which carries the stable isotope signature of the MOW moving into the Atlantic, gives us the opportunity to answer the following questions: how did northeast Atlantic climate change on millennial to centennial time scales during the penultimate glacial period? what was the impact on Mediterranean climate and its heat and freshwater budgets, how did these millennial-scale climate changes affected the Mediterranean overturning and MOW strength?

The analysis of benthic $\delta^{13}C$ at site U1389 led Sierro et al. (2020) to infer two periods of slow MOW and weak Mediterranean overturning circulation during MIS6 that occurred at times of maximum summer insolation in the northern Hemisphere. The timing of the first period event is coetaneous with the formation of the "glacial sapropel" S6 in the Mediterranean. Sapropels in the eastern Mediterranean reflect episodes of reduced bottom water ventilation. They have been associated to weak overturning circulation at times of decreasing sea surface densities in the areas of deep water formation due to fresh water input into the Mediterranean (Casford et al., 2003; Emeis et al., 2003; Grimm et al., 2015; Rohling et al., 2015). There are several sources of freshwater that could have preconditioned the Mediterranean for its final stagnation and sapropel formation: freshwater from African monsoons transported to the Mediterranean via Nile river; enhanced annual rainfall in peri-Mediterranean regions; entrance of an Atlantic inflow with lower salinities or meltwater from the Alpine glaciers (Casford et al., 2003; Emeis et al., 2003; Grant et al., 2016; Grimm et al., 2015; Rohling et al., 2002, 2015; Rossignol-Strick, 1983; Thunell and Williams, 1983; Troelstra et al., 1991). Although these different sources of freshwater are not mutually exclusive more evidences are needed to discriminate between them, especially during the formation of sapropel S6 during the penultimate glacial period.

The exceptional, high-resolution record from IODP site U1389 together with the analysis of surface water variations in other two cores near the entrance of the Mediterranean allowed to investigate what were the main mechanisms that preconditioned the Mediterranean during sapropel S6 formation.

2. Regional setting: the southern Iberian Margin

IODP site U1389 was drilled in the continental slope of the Gulf of Cadiz, around 100 km to the west of the Strait of Gibraltar. It is located along the main path of the MOW, which is the result of mixing of the Mediterranean outflow with East North Atlantic Central Water (ENACW) in the Gibraltar Strait. The higher density of the Mediterranean outflow today compared with the ENACW forced the MOW to rapidly descends into the Atlantic to reach its equilibrium depth between 500 and 1500 m, above the North Atlantic Deep Water (NADW) (Ambar and Howe, 1979; Sanchez-Leal et al., 2017) (Fig. 1). The fast flow of the MOW along the southern margin of Iberia interacts with bottom sediments to form the Gulf of Cadiz contourite system (Hernandez-Molina et al., 2016; Llave et al., 2001; Stow et al., 2013b).

The surface circulation in the area is dominated by the ENACW, which is characterized by the southward flow of the Portugal current and the Azores Current moving eastward in the southeast Iberian Margin (Peliz et al., 2005). The Atlantic inflow into the Mediterranean is fed by the ENACW (Peliz et al., 2009; Soto-Navarro et al., 2012) that after some mixing with Mediterranean water at the Strait of Gibraltar forms the Modified Atlantic Water (MAW) that flows mainly along the northern African margin to reach the eastern Mediterranean (Font et al., 1998).

The Iberian margin has been considered a key region for past climate change because of its potential to integrate the marine and terrestrial climate records, especially since the work of Shackleton et al. (2000) that was based on the isotope record recovered from core MD95-2042 located in the southwestern Portuguese margin, at the so-called Shackleton site. This area attracted great attention and several new cores have been drilled almost at the same position, i.e. core MD01-2444-2443 and IODP site U1385 (Hodell et al., 2013b; Martrat et al., 2007). All of them were located between 2500 and 3000 m water depth to investigate past changes in north Atlantic thermohaline circulation since the area was bathed by a) the NADW during periods of intense Atlantic Meridional Overturning Circulation (AMOC) in interglacial times and b) the Antarctic Bottom Water (AABW), which flows today at deeper depths along the Iberian margin, and was shallowed during glacial periods when the AMOC weakened (Hodell et al., 2013a; Martrat et al., 2007; Shackleton et al., 2000).

Our record in the Gulf of Cadiz does not allow a direct connection with the deep Atlantic circulation because it is located at a shallower depth within the path of the MOW and it is not affected by the NADW or AABW (Fig. 1). Due to this shallow position, the benthic $\delta^{18}O$ record was not used to establish the chronology for this site (see sections 5 and 7), instead, we used the planktic $\delta^{18}O$ that reflects surface water changes throughout the Iberian Margin.

3. Material and methods

This study is based on a high-resolution isotope record recovered from IODP site U1389 that was partially published in Sierro et al. (2020). This site was drilled in the southern Iberian Margin at 640 m water depth in the Gulf of Cadiz (36°25.515′N; 7°16.683′W) (Fig. 1) during IODP expedition 339 (Mediterranean Outflow). The interval from 63 to 120 m depth was sampled every 10 cm. The lithology mainly consists of a succession of mud and sandy-silt contourite beds (Stow et al., 2013a). Approximately 20 cc of sediment were dried, weighed, disaggregated in tap water and poured into a 62 μm sieve to remove the fine particles and this residue was dried and dry-sieved again using a 150 μm sieve.

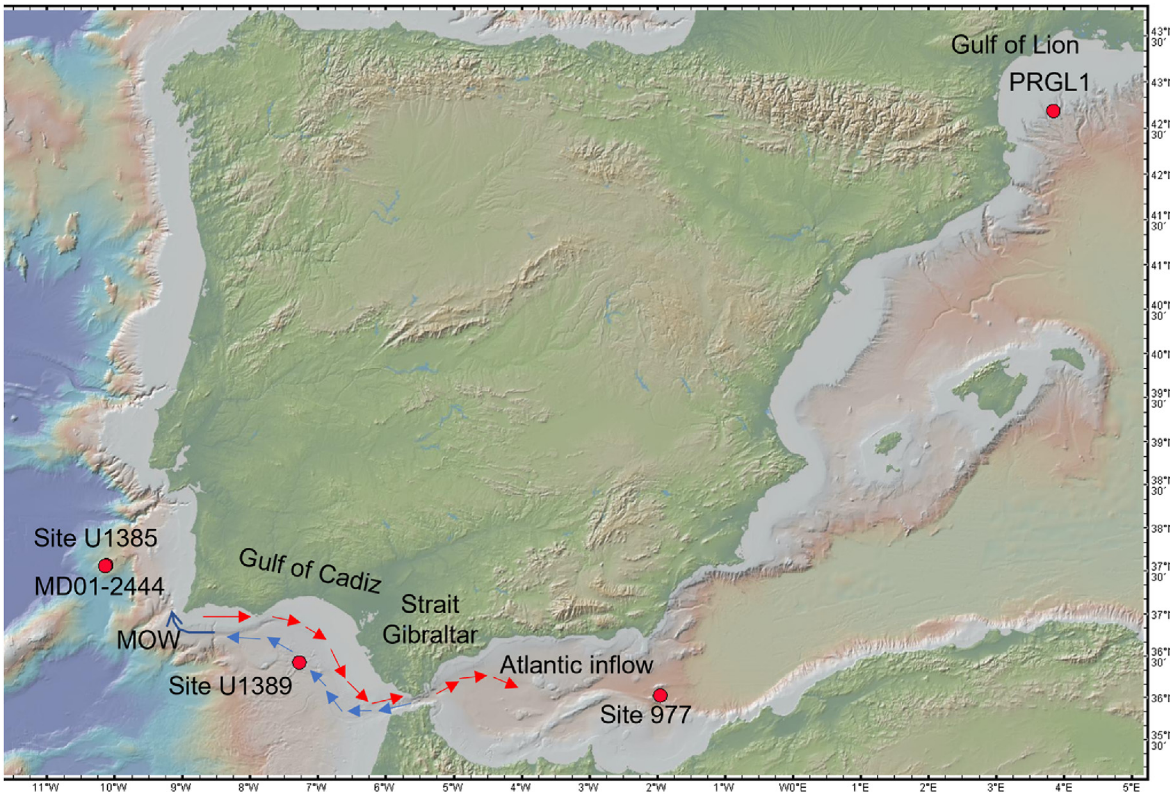

Fig. 1. Location of the sites studied and mentioned in this study. Blue arrows show the main trajectory of the MOW. Red arrows show the main path of the Atlantic inflow into the Mediterranean. Figure made with GeoMapApp (www.geomapapp.org). (For interpretation of the references to color in this figure legend, the reader is referred to the Web version of this article.)

Benthic oxygen isotope analyses were performed by using approximately 2–10 specimens of the benthic foraminifer species *Cibicidoides pachyderma* larger than 250 μm. The *G. bulloides* planktic $\delta^{18}O$ and *C. pachyderma* benthic $\delta^{13}C$ as well as the percentage of fine sand (weight percent of the fraction 62–150 μm relative to the bulk dry weight) data used in this study were previously published in Sierro et al. (2020).

We used data from site 977 and core PRGL1 to calculate the seawater $\delta^{18}O$ for these sites. Seawater $\delta^{18}O$ in site 977 was estimated by using the temperature-corrected, *G. bulloides* $\delta^{18}O$ record published by Martrat et al. (2004) and an ice volume correction of 0.009‰ per meter, using the sea level record of Grant et al. (2014). In the same way, sea surface $\delta^{18}O$ change during MIS6 was calculated for core PRGL1, drilled in the Gulf of Lion, using the temperature corrected *Globigerina bulloides* $\delta^{18}O$ record published by Sierro et al. (2009), the SST record of Cortina et al. (2015) and the same ice volume correction of 0.009‰ per meter, using the sea level record of Grant et al. (2014). For the correction of the SST effect we used the *G. bulloides* temperature ($\delta^{18}O$) equation of Bemis et al. (1998) T(°C) = 13.2-4.89*(δ_c-δ_w). Because the application of this equation gave $\delta^{18}O$ values of ~2‰ for the current seawater at site 977 with an average $\delta^{18}O$ of 1‰, we subtracted 1‰ from all estimated $\delta^{18}O$ values in the record to make them more comparable to the present. The same correction of −1‰ was applied to the seawater $\delta^{18}O$ estimations at site PRGL1.

4. Results

The benthic and planktic stable isotope records show similar trends (Fig. 2). The planktic $\delta^{18}O$ record was published in Sierro et al. (2020). Both records display long and short-term variability. High $\delta^{18}O$ values are observed in the lower part of the section, followed by low values until 103 mcd (meters composite depth). After this minimum, an upward increasing trend is observed ending with high and relatively constant values in the upper part of the section that culminates with a prolonged decrease in the uppermost part. The short-term variability is more visible in the planktic than in the benthic $\delta^{18}O$, especially in the middle part of the records.

The benthic $\delta^{13}C$ displays a completely different pattern, showing a cyclical behavior characterized by four intervals with high $\delta^{13}C$ followed by intervening intervals with low benthic $\delta^{13}C$. A complete record of benthic $\delta^{13}C$ for the last 250 ky was published in Sierro et al. (2020). In addition to this long-term cyclical behavior, short-term variability is also recognized in the benthic $\delta^{13}C$, especially in some of the intervals of high benthic $\delta^{13}C$.

The percentage of fine sand in the sediments retrieved from site U1389 also exhibits a cyclical behavior, similar to that observed in the benthic $\delta^{13}C$. Four intervals with higher fine sand contents and high benthic $\delta^{13}C$ are followed by intervals with low fine sand and low benthic $\delta^{13}C$ (Fig. 2). Short-term variability is also visible in the fine sand content that covaries with the benthic $\delta^{13}C$. A record of fine sand for the last 250 ky was published in Sierro et al. (2020), in this study we focused on the variability observed during MIS6.

5. Alignment of millennial-scale variability of site U1389 with the hydrogen isotope record from EPICA dome C

To elaborate a chronology for site U1389 we first followed the age model published by Sierro et al. (2020) that was based on the alignment of the planktic $\delta^{18}O$ to the Greenland synthetic $\delta^{18}O$ record (Barker et al., 2011) for the last 250 ky (Sierro et al., 2020).

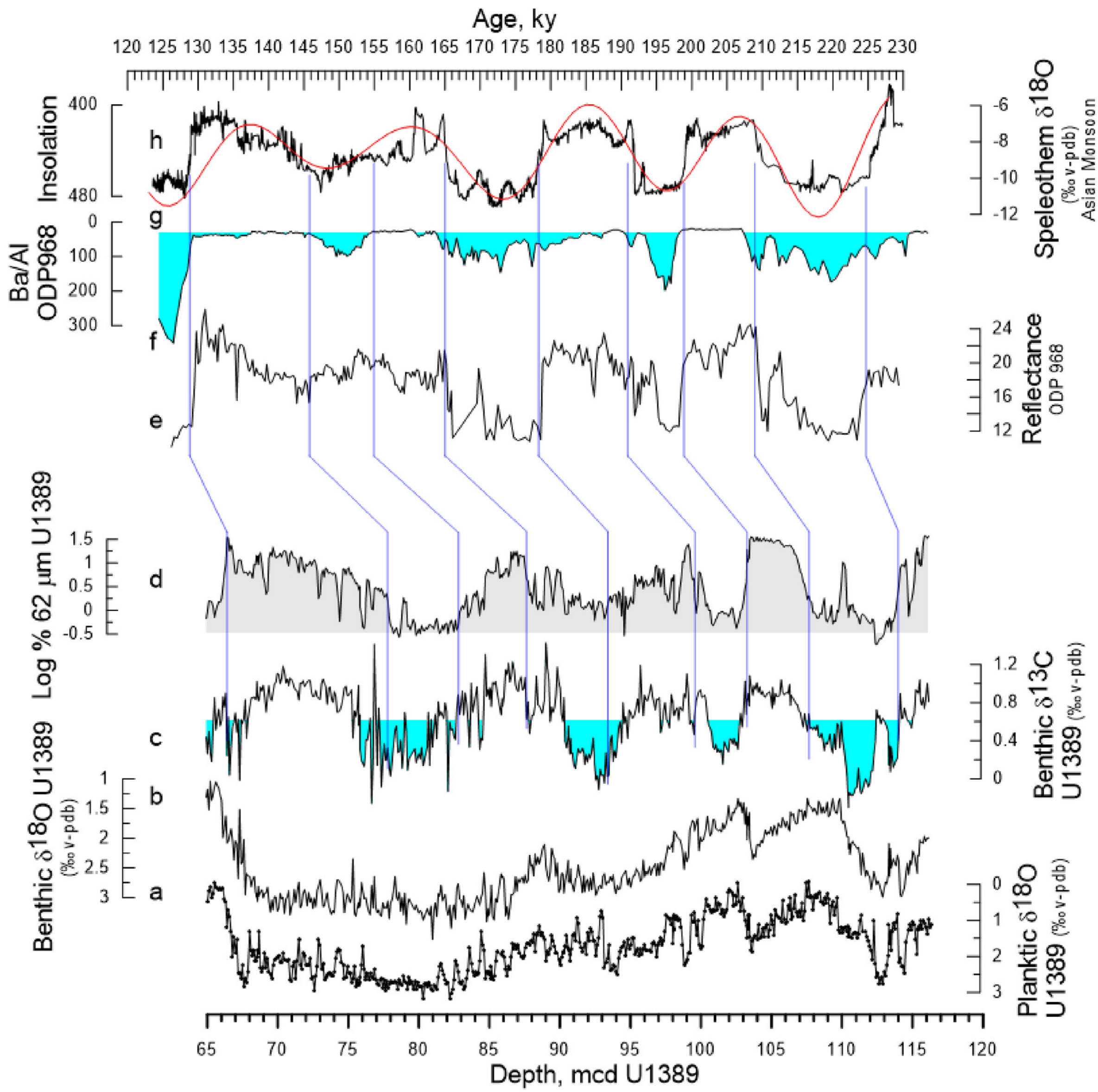

Fig. 2. Plot of planktic and benthic stable isotope records and fine sand percent (fraction 62–150 μm) versus depth at site U1389, showing the tie points used for alignment with eastern Mediterranean sapropels (ODP site 968) (Ziegler et al., 2010) and the Speleothem $\delta^{18}O$ record of East Asian Monsoons (Cheng et al., 2016): **a**) Planktic $\delta^{18}O$, **b**) benthic $\delta^{18}O$ and **c**) benthic $\delta^{13}C$ records from IODP site U1389. **d**) Percent fine sand (62–150 μm) from IODP site U1389. **e**) Sediment reflectance and **f**) Ba/Al records from ODP site 968 in the Eastern Mediterranean (Ziegler et al., 2010). **g**) Northern Hemisphere summer insolation (Laskar et al., 2004). **h**) Speleothem $\delta^{18}O$ record of East Asian Monsoons (Cheng et al., 2016).

Based on the high reproducibility of the planktic oxygen isotope records along the southern Iberian Margin, the oxygen isotope records from MD01-2444 and IODP site U1389 for the penultimate glaciation were aligned (Fig. 3). Once the planktic $\delta^{18}O$ records were synchronized, we used the age scale of Margari et al. (2010) for MD01-2444 that was based on the alignment of the benthic $\delta^{18}O$ in that core and the δD from EPICA dome C (EDC), using the AICC2012 chronology (Bazin et al., 2013). This is important because the improved temporal resolution of site U1389 allowed the identification of centennial to millennial changes not visible in MD01-2444. Following Shackleton et al. (2000), the benthic oxygen isotope record from core MD01-2444 has been directly linked to millennial-scale air temperature in Antarctic ice cores during MIS 6 (Margari et al., 2010) based on the great similarity between the benthic $\delta^{18}O$ in the Iberian Margin and the δD record from Antarctica, which is the best proxy for air temperature in that region. This similarity probably comes from the straight coupling between Antarctic air temperature and global ice volume (Shackleton et al., 2000). However, since the benthic $\delta^{18}O$ record from the Gulf of Cadiz mainly reflects past changes in the temperature and oxygen isotope signature of the MOW, we can now connect the centennial to millennial climate changes recorded at site U1389 with deep water thermohaline circulation in the Atlantic and the Antarctic ice core records for the penultimate glaciation (Fig. 3). Thus, for the global connection to the deep ocean circulation we used the well-established correlation between the benthic $\delta^{18}O$ record from core MD01-2444 and the Antarctic ice core record on the AICC2012 chronology (Fig. 3).

6. Millennial-scale climate variability during MIS6 in the NE Atlantic

As the penultimate glaciation progressed, the SST of the Iberian margin, including the southern margin of the Iberian Peninsula in

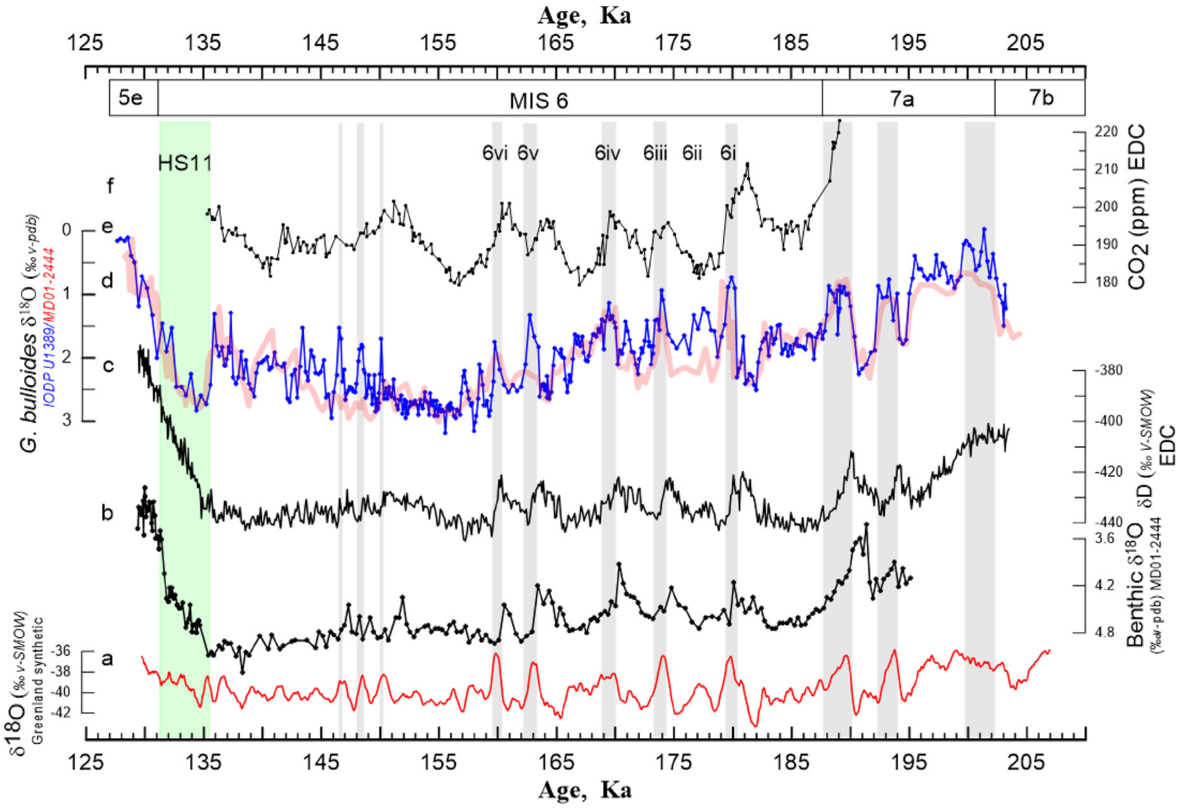

Fig. 3. Alignment of the U1389 (Sierro et al., 2020) and MD01-2444 (Margari et al., 2010) *G. bulloides* $\delta^{18}O$ records with the Greenland synthetic record (Barker et al., 2011) and δD in Antarctica (Jouzel et al., 2007). All records are plotted on the AICC2012 time scale. **a**) Greenland synthetic record (Barker et al., 2011). **b**) benthic $\delta^{18}O$ record from MD01-2444 (Margari et al., 2010). **c**) δD from Epica Dome C, Antarctica (Jouzel et al., 2007). **d**) *G. bulloides* $\delta^{18}O$ from IODP site U1389 (blue) (Sierro et al., 2020). **e**) *G. bulloides* $\delta^{18}O$ from core MD01-2444 (pink) (Margari et al., 2010). **f**) CO_2 from EDC (Shin et al., 2020). Grey bars show *G. bulloides* $\delta^{18}O$ minima. (For interpretation of the references to color in this figure legend, the reader is referred to the Web version of this article.)

the western Mediterranean experienced a long-term trend of cooling (Martrat et al., 2004, 2007) (Figs. 3 and 4) that is reflected in the planktic $\delta^{18}O$ record in core MD01-2444 (Hodell et al., 2013a; Margari et al., 2010). Due to the strong similarities between the U1389 and MD01-2444 $\delta^{18}O$ records, we assumed that oxygen isotope millennial change at site U1389 was also mainly controlled by SST (Figs. 3 and 4).

In general, the long-term cooling trend between 200 and 150 ky can be divided in several sequences limited by major warming interstadial events recorded by major drops in the planktic $\delta^{18}O$ in site U1389 and core MD01-2444 (Figs. 3 and 4). Each sequence is formed by two to four interstadial/stadial events as can be seen for example between warming events 6v and 6iv (Figs. 3 and 4). The overall $\delta^{18}O$ trend is similar in U1389 and MD91-2444, but additional centennial to millennial-scale $\delta^{18}O$ changes can be seen in site U1389 that are not visible in the Shackleton site oxygen isotope record. This pattern reminds the sequences of Dansgaard-Oeschger interstadial/stadial events (Dansgaard et al., 1993; Johnsen et al., 1992), culminating in progressively cooler stadials in the last glacial period (Bond et al., 1993; Bond and Lotti, 1995), although the cooling episodes at the end of these sequences are not related to Heinrich stadials in MIS6. The average duration of these sequences is similar to those in MIS3, ranging between 4000 and 9000 yr (Fig. 4). As already reported by Margari et al. (2010), the prominent warming events at the onset of these sequences are contemporaneous with maximum air temperature in Antarctica and the highest CO_2 in the atmosphere, as recorded in EDC records (Jouzel et al., 2007; Shin et al., 2020). In contrast, CO_2 and air temperature in Antarctica increases during the colder stadials towards the final stages of the sequences (Fig. 3). This behavior has been related to millennial-scale changes in interhemispheric ocean heat transport (Shin et al., 2020). The major warming events are linked to the onset of an intense AMOC that transferred warm water to the north Atlantic, at least to the latitude of ODP site 983 (Barker et al., 2019) as may be seen by the abrupt decreases in abundance of the polar species *Neogloboquadrina pachyderma* (Fig. 4). This strong AMOC certainly increased heat transport to the north, causing the gradual drop in temperature seen in hydrogen isotope records in Antarctic ice cores (Jouzel et al., 2007; Bazin et al., 2013). These warming events were also recorded in the pollen assemblages that reflect higher air temperatures and higher percentages of temperate trees along Southern Portugal (Margari et al., 2010; Tzedakis et al., 2018) (Fig. 4).

This rapid variability at site U1389 differs from that observed in higher latitudes during the penultimate glaciation based on records of hematite stained grains contents (Obrochta et al., 2014). The last authors found a reduced millennial-scale variability during MIS 6 compared with that seen in the last glacial period and within MIS8.

The millennial-scale variability is more regular and frequent along the phase of ice sheet growth during the penultimate glaciation. This is similar to what has been observed during the last glacial age when the period with more regular stadial-interstadial oscillations occurred during the main phase of ice sheet growth preceding the last glacial maximum. All this points to the interaction between ocean-atmosphere-ice sheets as the main control of millennial-scale variability (Mitsui and Crucifix, 2017). The number of warming transitions recorded by the *G. bulloides* $\delta^{18}O$ at site U1389 is higher than that observed in the SST records from core

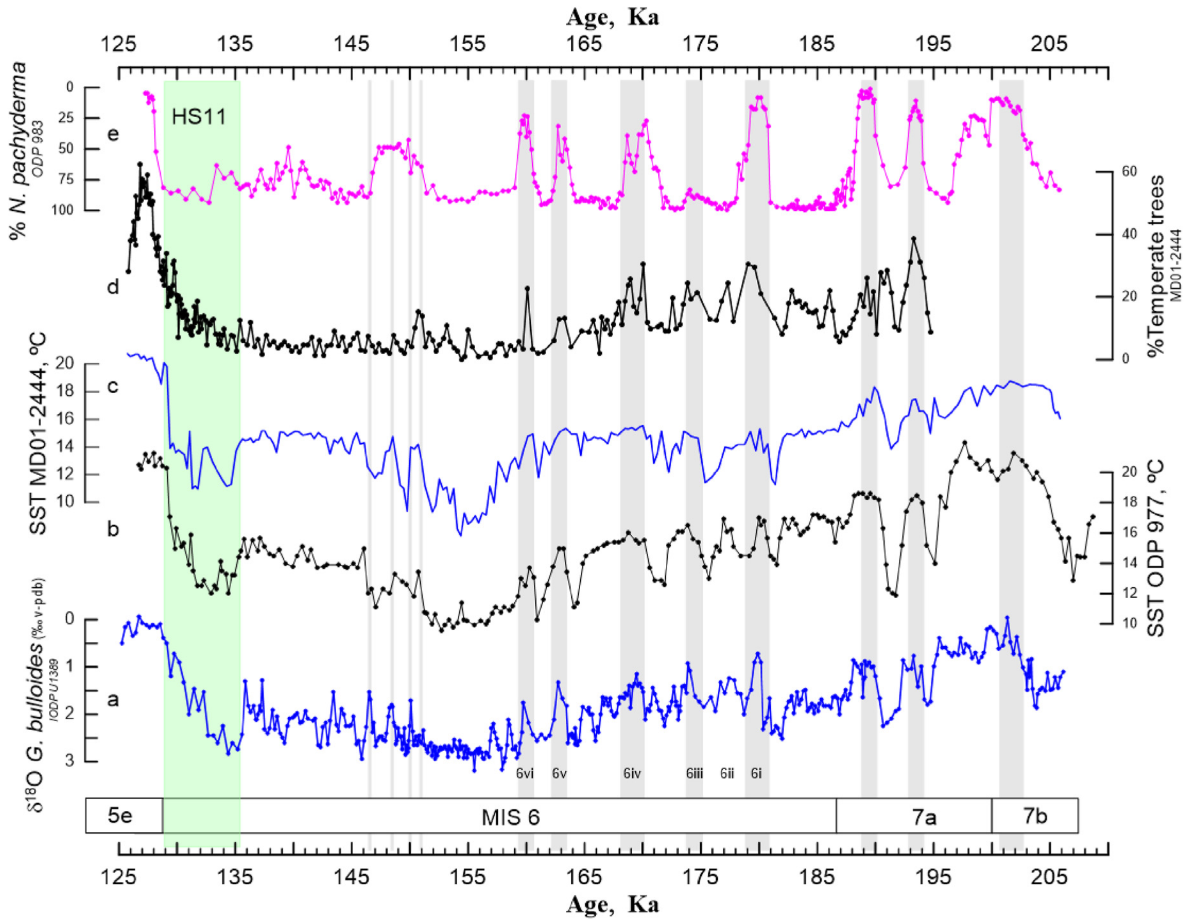

Fig. 4. Millennial-scale climate changes during MIS6 in the north Atlantic and western Mediterranean. **a)** *G. bulloides* $\delta^{18}O$ from U1389 (Sierro et al., 2020). **b**) Sea surface temperature from ODP site 977 (western Mediterranean) (Martrat et al., 2004). **c**) Sea surface temperature from core MD01-2444 (Portuguese margin) (Martrat et al., 2007). **d**) Record of percent temperate tree pollen from core MD01-2444 (Margari et al., 2014; Tzedakis et al., 2018). **e**) Record of relative abundance of *Neogloboquadrina pachyderma left* from site ODP 983 in the north Atlantic (Barker et al., 2015, 2019). Grey bars show *G. bulloides* $\delta^{18}O$ minima during some of the major interstadial periods. All records are plotted on the AICC2012 time scale with the exception of the *N. pachyderma* abundance from site 983, which is plotted on its own time scale (Barker et al., 2019).

MD01-2444 and ODP site 977 (Martrat et al., 2004, 2007), which may be explained by the short duration of some of the events and the lower sedimentation rates of these records that did not allowed high-resolution studies.

In contrast to this period of high variability, climate was more stable towards the glacial maximum. This was a period of severe climate cooling, lasting for a few millennia that was recorded in the NE Atlantic and western Mediterranean (Margari et al., 2010; Martrat et al., 2004) (Fig. 4). SST as low as 8 °C were reached in the Southwest Iberian margin (Martrat et al., 2007) and 10 °C in the western Mediterranean (Martrat et al., 2004) and these cool waters were accompanied by abundant polar species in the north Atlantic (Barker et al., 2019). Significant melting in the southern margin of the Fennoscandian ice sheets is recorded by a notable increase in meltwater and terrigenous supply to the Gulf of Biscay through the Channel River that coincided with the coalescence of the British-Irish and Fennoscandian ice sheets (Boswel et al., 2019; Eynaud et al., 2007; Toucanne et al., 2009). Indeed, terrigenous supply to the Gulf of Biscay was higher than that observed during Termination II probably due to ice retreat in the southern margin of the Fennoscandian ice sheets (Boswel et al., 2019; Penaud et al., 2009; Toucanne et al., 2009).

The transition from this cold period to a warmer NE Atlantic during the glacial maximum is recorded in the Gulf of Cadiz by a series of interstadial/stadial events identified in the planktic $\delta^{18}O$ record (Fig. 4), although the isotope data are more noisy in this part of the record. During this time period warmer surface waters are also recorded in the north Atlantic at site 983 by drops in abundance of *N. pachyderma* (Barker et al., 2019) (Fig. 4), suggesting enhanced northward heat flow. However, these short-term warming events in the Ocean do not seem to be recorded in the pollen assemblages in MD01-2444 (Margari et al., 2010) (Fig. 4), although this could be related to the lower resolution of these records.

7. Alignment of millennial climate change with Asian monsoon records across MIS6

Between MIS7 and MIS6 Sierro et al. (2020) identified four episodes of weak MOW at site U1389 that were linked to sapropel events in the eastern Mediterranean (Fig. 2). They were identified by low fine sand content and low benthic $\delta^{13}C$ at site U1389. This synchronism between MOW weakening events in the Gulf of Cadiz and the timing of eastern Mediterranean sapropels give us the opportunity to elaborate a new chronology for MIS6 within the framework of the astronomically tuned time scale, which is based on the tuning of sapropels with Astronomical equations (Hilgen et al., 2012).

The use of fine sand percent in the sediments as a proxy for MOW intensity is well established in the scientific literature (Bahr et al., 2015; de Castro et al., 2021; Kaboth et al., 2016; Llave et al., 2006; Sierro et al., 1999, 2020; Toucanne et al., 2007; Voelker et al., 2006). Lower sand contents are linked to episodes of weak MOW. In the same way, periods of weak MOW are recorded by low benthic $\delta^{13}C$ in the Gulf of Cadiz associated to weak overturning circulation in the Mediterranean, especially during sapropel formation (see Sierro et al., 2020 for more detail). However, the benthic $\delta^{13}C$ at site U1389 also depends on the mixing of the usually high $\delta^{13}C$ values of the outflowing water and the lower $\delta^{13}C$ of the ENACW, being the last one especially low during times of weak AMOC. For this reason, in case of discrepancy between the two proxies we prefer to use the fine sand content that is more directly related to MOW strength.

Between MIS 5 and MIS7, sapropels S5, S6, S7 and S8 were deposited in the eastern Mediterranean, all of them are characterized by darker colors (low reflectance) and high Ba/Al (Ziegler et al., 2010; Konijnendijk et al., 2014). The low reflectance and high Ba/Al ratios in the eastern Mediterranean reflect high organic matter contents in the sediments usually related to stagnation events during sapropel deposition (Ziegler et al., 2010; Konijnendijk et al., 2014). To elaborate our new chronology, the prominent episodes of low benthic $\delta^{13}C$ and minimum fine sand content at site U1389 were aligned with sapropels S5, S6 and S7 characterized by high Ba/Al and low reflectance in ODP site 968 in the eastern Mediterranean (Ziegler et al., 2010; Konijnendijk et al., 2014) (Fig. 2). A prominent decrease in fine sand and benthic $\delta^{13}C$ in the Gulf of Cadiz during the glacial maximum of MIS6 have no sapropel equivalent in the Mediterranean but it could be aligned with an event of high Ba/Al at site 968 (Fig. 2). For the alignment of this episode we prefer to correlate the minimum of fine sand with the interval of high Ba/Al at site 968 because the benthic $\delta^{13}C$ at site U1389 could be influenced by the mixing of a weak MOW flow with a larger volume of ^{13}C depleted intermediate water in the Atlantic due to the weak AMOC during this time.

Because sapropels were triggered by events of strong tropical monsoons they have been tuned to maximum northern Hemisphere summer insolation (Ziegler et al., 2010; Konijnendijk et al., 2014) and calibrated with the radiometrically dated Asian monsoon speleothem records (Cheng et al., 2016). Following this approach, we placed the millennial-scale climate variability retrieved from site U1389 in the chronologic framework of the astronomical time scale (Ziegler et al., 2010; Konijnendijk et al., 2014) and the radiometric scale of Asian monsoon speleothem records (Cheng et al., 2016). For Termination II we used the age scale of Marino et al. (2015) based on the common patterns of variability between the Mediterranean and MD01-2444 planktic $\delta^{18}O$ records and the $\delta^{18}O$ speleothem records from Corchia (Italy).

When comparing the chronology based on the alignment of the Iberian margin $\delta^{18}O$ and Antarctic EDC δD records with the AICC2012 age scale (Bazin et al., 2013; Veres et al., 2013) with that based on the alignment with Asian monsoons (Cheng et al., 2016) an offset of 1–5 ky emerges between the two chronologies (Fig. 5). Overall, the ages based on the Monsoon chronology are younger, especially the age of events during the glacial maximum (Fig. 5).

The AICCC2012 chronology (Bazin et al., 2013; Veres et al., 2013) has been revised recently by Extier et al. (2018) based on the great resemblance between the atmospheric $\delta^{18}O$ of the air trapped in EDC ice cores and the Asian $\delta^{18}O$ speleothem record (Cheng et al., 2016) and the link of both records with the low latitude water cycle and astronomical precession. Declines of the EDC atmospheric $\delta^{18}O$ have been related to northward shifts of the intertropical convergence zone and the enhanced tropical monsoons during precession minima (summer insolation maxima) due to higher precipitation in the mid latitudes of the northern Hemisphere (Landais et al., 2010; Extier et al., 2018). The average $\delta^{18}O$ of precipitation decreases because of the amount effect and these decreases are transmitted to the atmosphere via terrestrial vegetation photosynthesis, which is further stimulated during these periods of higher annual rainfall (Goni et al., 2008), emitting more depleted oxygen to the atmosphere at times of summer insolation maxima (Extier et al., 2018; Landais et al., 2010). If the tuning of the fine sand percent with monsoon speleothems and the alignment of MD01-2444 benthic $\delta^{18}O$ and Antarctic δD records are correct, then the Antarctic AICC2012 chronology should be shifted to younger ages (Fig. 5). Our new Monsoon chronology for millennial variability during MIS6 at site U1389 supports the new EDC chronology of Extier et al. (2018) since the timing of the low fine sand content and low benthic $\delta^{13}C$, which depict weak Mediterranean overturning at times of summer insolation maxima (precession minima), are more in phase with the periods of lower atmospheric $\delta^{18}O$ in Antarctic EDC (Fig. 5).

8. Impact of millennial scale climate change on Mediterranean overturning and MOW strength

Unlike the planktic $\delta^{18}O$, which provides an exceptional record of climate change in the NE Atlantic, the benthic $\delta^{18}O$ and $\delta^{13}C$ in the Gulf of Cadiz carries the Mediterranean climate signature because bottom waters at the position of site U1389 were bathed by the MOW.

The straight coupling between planktic and benthic $\delta^{18}O$ at site U1389 revealed that almost all the abrupt oxygen isotope changes recorded in the planktic species are also recorded in the benthic forms, although the amplitude in bottom waters is smaller. This unambiguously revealed that the millennial climate change variability recorded in the NE Atlantic also affected the Mediterranean, including the eastern Mediterranean, which is the main source of the MOW.

Although MOW strength and Mediterranean overturning are mainly controlled by precession-driven changes in Mediterranean freshwater and heat budgets as emphasized in the previous section, the impact of interstadial-stadial climate events is clearly visible in both the fine sand content and the benthic $\delta^{13}C$ (Fig. 6) as reported for MIS 3–5, especially during the periods of summer insolation minima when, on average, a high intensity MOW is recorded. Conversely, during summer insolation maxima characterized by weak average MOW the impact of millennial-scale interstadial/stadial events is small and sometimes is hardly visible. However, during the three periods of insolation minima when the MOW was stronger and Mediterranean overturning circulation was enhanced, all interstadial events are linked to MOW weakenings and reduced Mediterranean overturning, as may be inferred from the lower percentages of fine sand in the sediments and drops of the benthic $\delta^{13}C$ (Fig. 6). The most prominent weakening events of Mediterranean overturning and drops in MOW strength are recorded during the major warming events occurring during the insolation minima (Fig. 6).

All this indicates that millennial-scale climate events resulting from reorganizations of the Atlantic meridional overturning circulation also had a strong impact on Mediterranean climate and its hydrologic budget. These interstadial MOW weakening events certainly reflect warmer winter air temperatures on the northern margins of the Mediterranean and/or lower net freshwater loss resulting in lower surface seawater salinities and densities in the areas of intermediate water formation.

The main trend of the benthic $\delta^{18}O$ follows the global pattern of sea level change as may be seen in Fig. 6, however, multiple millennial-scale oxygen isotope deviations from the global eustatic pattern are recorded, coinciding with the planktic $\delta^{18}O$ millennial variability. Overall, while the planktic $\delta^{18}O$ and benthic $\delta^{13}C$

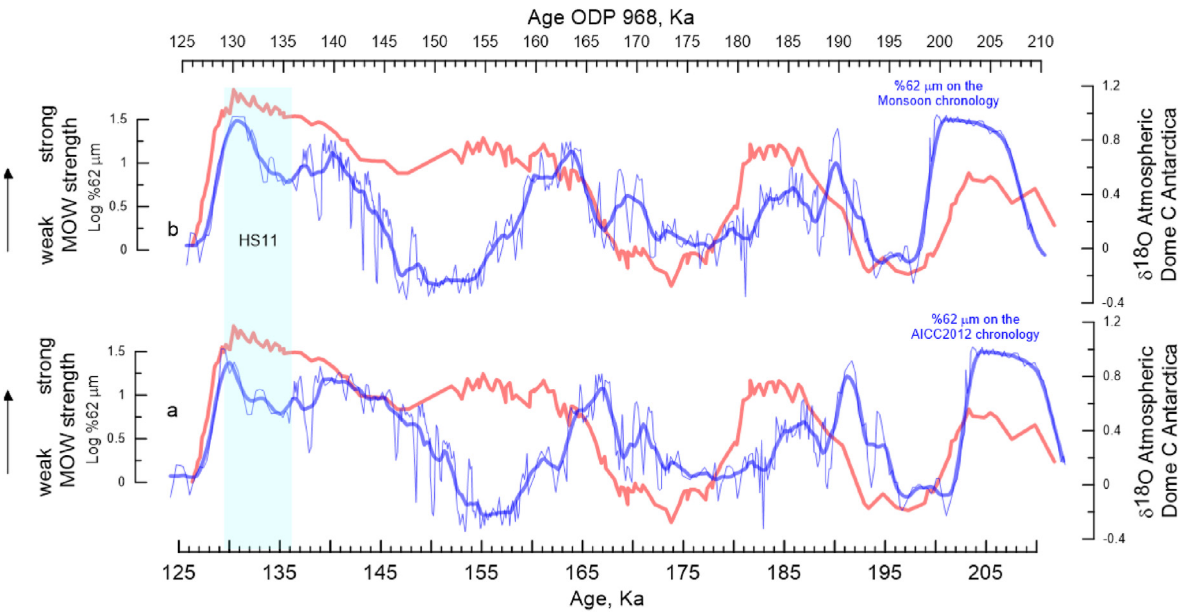

Fig. 5. Comparison of Precession-driven variations in MOW strength inferred from Log % 62 μm in IODP site U1389 (blue lines) and atmospheric $\delta^{18}O$ from EDC Ice Core (Extier et al., 2018) (red line). **a**) Log % 62 μm plotted on the AICC2012 time scale. **b**) Log % 62 μm plotted on the Monsoon chronology. Thick blue line shows the 2 ky moving average of the log % 62 μm record. (For interpretation of the references to color in this figure legend, the reader is referred to the Web version of this article.)

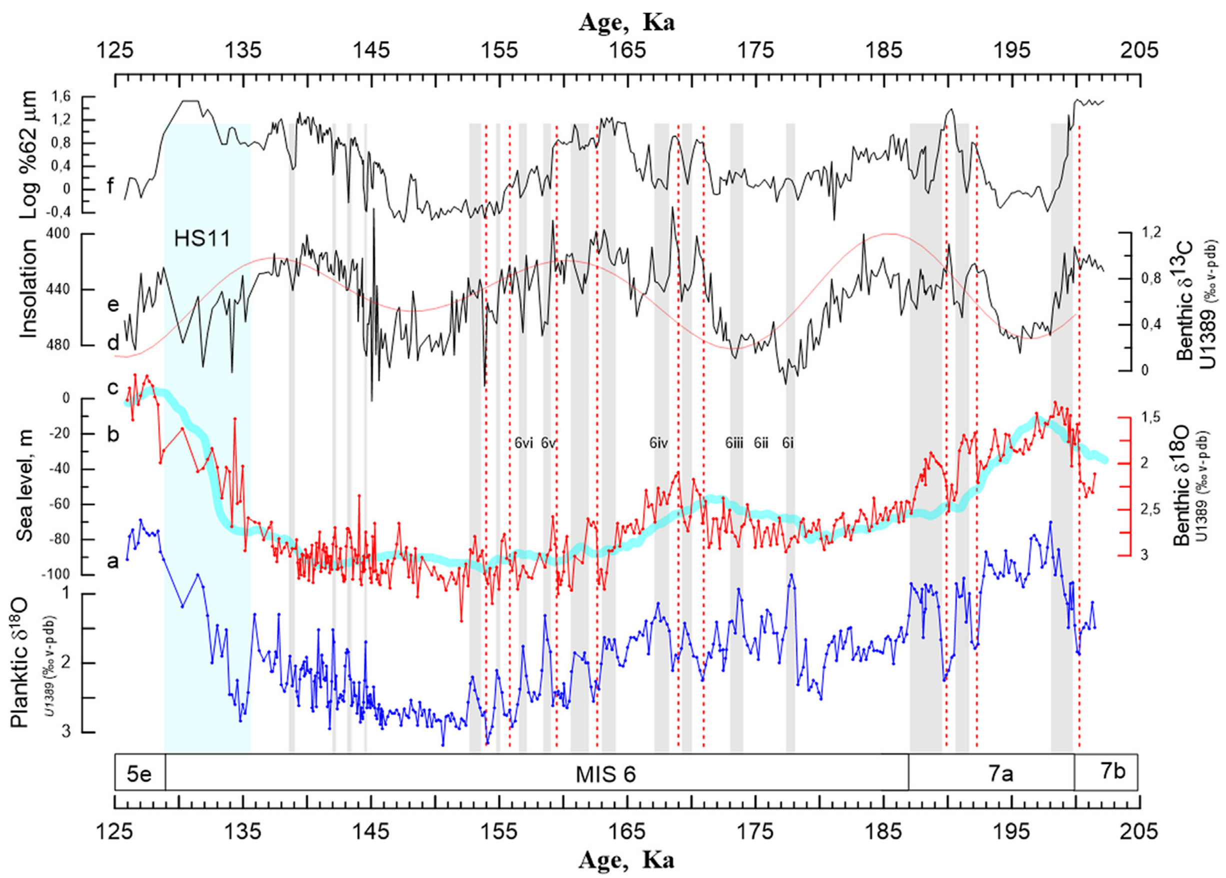

Fig. 6. Impact of Millennial-scale climate variability on eastern Mediterranean climate during the penultimate glacial period. **a)** Planktic $\delta^{18}O$ record from IODP site U1389. **b**) Benthic $\delta^{18}O$ record from IODP site U1389 (in red). **c**) Global sea level change (in blue) after Grant et al. (2014). **d**) Northern Hemisphere Summer insolation (in red) (Laskar et al., 2004). **e**) Benthic $\delta^{13}C$ record from IODP site U1389. **f**) Percent fine sand at site U1389 expressed as weight% of the fraction (62–150 μm) in logarithmic scale. Grey bars show interstadials periods as depicted by planktic $\delta^{18}O$ minima. Red dashed lines indicate benthic $\delta^{18}O$ drops that precede planktic $\delta^{18}O$ drops by a few hundred years. Marine oxygen isotope stages are shown for reference. All records are plotted on our new Monsoon chronology. (For interpretation of the references to color in this figure legend, the reader is referred to the Web version of this article.)

occurred in phase, as described above, a lag between the benthic $\delta^{18}O$ millennial changes and the planktic $\delta^{18}O$ was recognized. This phase lag between the benthic and planktic $\delta^{18}O$ at site U1389 was probably the result of the mixture of Mediterranean outflowing water and Atlantic intermediate water that takes place in the Strait of Gibraltar. Because the Mediterranean outflowing water is warmer than the Atlantic intermediate water, benthic foraminifers calcifying under the influence of the MOW will show lower $\delta^{18}O$ values than those living under the influence of intermediate Atlantic water, even though the $\delta^{18}O$ of the MOW is higher. Therefore, after mixing the Mediterranean and Atlantic water at the Strait of Gibraltar, the $\delta^{18}O$ of benthic foraminifers along the path of the MOW depends on the proportions of the warmer Mediterranean Outflow and the colder Atlantic water as well as on the $\delta^{18}O$ of both water masses. This mixture of Mediterranean and Atlantic water at the Strait of Gibraltar probably changed as a function of the strength of the MOW that led to a higher proportion of the warmer Mediterranean water when the MOW got stronger. In addition, the physical-chemical properties of the Mediterranean Outflow also changed with time. Winter cooling in the eastern Mediterranean during stadial events should have cooled the intermediate Levantine water and therefore lowered the temperature of the Mediterranean Outflow. Cooling events of 2 °C were recorded in the deep Mediterranean water during some stadials in MIS3 (Cacho et al., 2006). In the same way, a drier Mediterranean climate should have generated a more saline and higher $\delta^{18}O$ outflow due to the preferential evaporation of the light ^{16}O isotope during stadial periods. Conversely, during interstadial periods, a warmer and lighter outflow would be expected. If changes in the benthic $\delta^{18}O$ were only the result of changes in Mediterranean water properties, the benthic and planktic $\delta^{18}O$ at site U1389 would have to be in phase. Indeed, this pattern is seen during the two stadial interstadial periods in MIS 7a, a strengthened MOW during the prominent stadial period centered at around 190 ky is recorded by heavy ^{18}O benthic values (Fig. 6), suggesting that Mediterranean climate was controlling the chemical signatures of the MOW in the Gulf of Cadiz. However, during the interstadial periods of MIS 6 when warmer waters and lighter ^{18}O planktic values are recorded in the Gulf of Cadiz, the benthic $\delta^{18}O$ decreased in parallel with a weaker MOW as recorded by falls in the benthic $\delta^{13}C$ and decreases of percent fine sand in the sediments (Fig. 6). A hotter and more humid Mediterranean climate should have generated a warmer and lighter oxygen isotope MOW, but instead heavier benthic oxygen isotope values are recorded. This apparent paradox can be explained by changing the mixing rates of Mediterranean and Atlantic waters in the Strait of Gibraltar, especially if the temperature difference between the Mediterranean Outflow and the Atlantic intermediate water was high. The MOW weakening during interstadials, clearly seen in the decreasing fine sand and drops of the benthic $\delta^{13}C$, reduced the transport of warm waters to the Atlantic and therefore a higher proportion of the colder Atlantic water is recorded at site U1389, causing the increases of the benthic $\delta^{18}O$. Although a lower benthic $\delta^{18}O$ is expected because of the wetter and warmer Mediterranean climate, this signature was probably counterbalanced by the larger impact of the colder temperature of bottom waters due to a lower proportion of the warmer MOW in relation to the colder Atlantic water. The declines of the benthic $\delta^{18}O$ normally occurred during phases of strong MOW towards the end of stadial events, clearly preceding the abrupt warming at the stadial interstadial transitions. A clear lag between falls of benthic and planktic $\delta^{18}O$ is observed, which is in the order of 200–400 yr (Fig. 6). These abrupt declines of the benthic $\delta^{18}O$ may reflect bottom water warming because of the enhanced heat transport from the Mediterranean at times of intense MOW, even though Mediterranean intermediate water was still cold at that time, but probably warmer than the Atlantic intermediate water. Mg/Ca measurements or clumped isotopes on benthic foraminifera are needed to further investigate millennial-scale bottom water temperature at this site.

The millennial-scale climate variability observed in the MOW is supported by other Mediterranean speleothem and pollen records showing the alternation of warm/humid periods and cold/arid episodes, similar to the intestadial/stadial events described above (Koltai et al., 2017; Nehme et al., 2018; Pickarski and Litt, 2017; Regattieri et al., 2021; Roucoux et al., 2011; Wainer et al., 2011, 2013; Wilson et al., 2021).

9. Influence of meltwater from the ice sheets on Mediterranean overturning circulation and formation of the “glacial sapropels”

Unlike most of the sapropels that were registered in warm periods, sapropel S6 was deposited during the penultimate glaciation (Ziegler et al., 2010) (Fig. 2). The extremely weak Mediterranean overturning circulation during this time is reflected by a prominent drop in benthic $\delta^{13}C$ at site U1389 in the Gulf of Cadiz (Sierro et al., 2020). A second drop in benthic $\delta^{13}C$ is recorded at site U1389 centered circa 150 ky that is linked to another episode of weak Mediterranean overturning, although in this case bottom waters from the eastern Mediterranean never reached complete anoxic conditions and no sapropel was deposited.

Bottom water anoxia during sapropel formation is linked to lower rates of deep water formation in the eastern Mediterranean caused by freshwater input from different sources e.g. river Nile, Black Sea, Mediterranean rainfall, meltwater inflow from the Atlantic, the Black Sea or from the Alpine ice sheets (Casford et al., 2003; Grimm et al., 2015; Rohling et al., 2015; Ziegler et al., 2010).

The growth of the Eurasian ice sheets during MIS 6 (the Saalian glaciation) started at around 197 ky and ended with a complete deglaciation at around 129 ky (Batchelor et al., 2019; Hughes et al., 2006; Inge et al., 2004; Mangerud et al., 2004). However, this growth was not continuous as referred in the previous sections, two episodes of meltwater caused by the partial retreat of the ice sheets were recorded in the NE Atlantic during MIS 6 by large accumulation rates of detrital material caused by retreat of the southwestern margin of the Eurasian ice sheets (Boswel et al., 2019; Eynaud et al., 2007; Toucanne et al., 2009). Both of them occurred at times of maximum summer insolation and are related to a smaller ice volume of the European ice-sheets (Bintanja and Van de Wal, 2008). Contemporaneous meltwater events were also recognized in the southeastern margin of the European icesheets that released meltwater to the Black Sea (Badertscher et al., 2011; Wegwerth et al., 2014, 2020). These meltwater events seem to be related with times of incomplete deglaciation as proposed by (Tzedakis et al., 2017).

To investigate the impact of these meltwater events on Mediterranean circulation and sapropel formation, we calculated the surface water $\delta^{18}O$ at ODP site 977 located in the Alboran Sea at the entrance of the Mediterranean (see methods) (Fig. 7). The surface water $\delta^{18}O$ in the Alboran sea carries the oxygen isotope imprint of the Atlantic inflow (LeGrande and Schmidt, 2006; Pierre, 1999; Voelker et al., 2015). Two periods of low surface water $\delta^{18}O$ were recognized at site 977 centered at 175 and 150 ky, coinciding with two periods of extreme weak Mediterranean overturning circulation as inferred from the low fine sand content and reduced benthic $\delta^{13}C$ (Fig. 7).

The timing of the first surface water $\delta^{18}O$ drop is equivalent to the onset of sapropel S6 in the eastern Mediterranean (Fig. 7) and the organic rich layer ORL A8 in the western Mediterranean (Comas et al., 1996). To investigate the spread of this meltwater into the

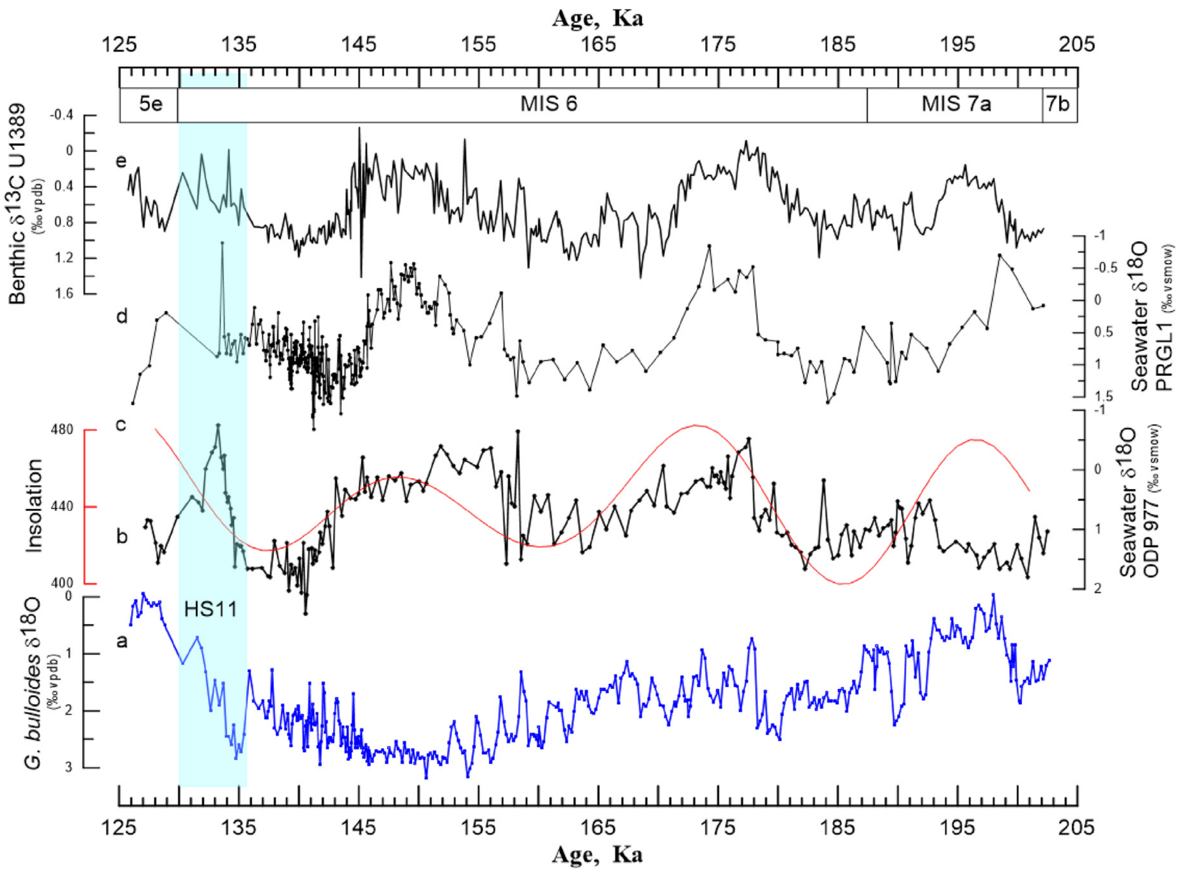

Fig. 7. Meltwater episodes in the Mediterranean during MIS6. **a.** Planktic $\delta^{18}O$ from site U1389 **b.** Seawater $\delta^{18}O$ from ODP site 977 (this study). **c.** Seawater $\delta^{18}O$ from borehole Promess PRGL1 (this study). **d.** Benthic $\delta^{13}C$ at site U1389 as a proxy for Mediterranean overturning (Sierro et al., 2020). All records are plotted on the new Monsoon chronology.

Mediterranean we calculated the seawater $\delta^{18}O$ in borehole PRGL1 in the Gulf of Lion (NW Mediterranean) (Fig. 7), which is a region where the Atlantic modified water entering from Gibraltar is well mixed with Mediterranean water today. The two prominent drops in the sea surface $\delta^{18}O$ seen at site 977 are also recognized in borehole PRGL1 in the Gulf of Lion. In particular, the amplitude of the $\delta^{18}O$ decrease centered at 175 ky is even higher than that recorded during MIS7 and the same prominent negative oxygen isotope excursion is also recorded in the planktic $\delta^{18}O$ from the Adriatic sea (Piva et al., 2008). A similar prominent contemporary drop in sea surface $\delta^{18}O$ has been widely recognized in the eastern Mediterranean at the onset of sapropel S6 (Casford et al., 2003; Emeis et al., 2003; Kallel et al., 2000; Schmiedl et al., 2003; Thunell et al., 1983) and in speleothem $\delta^{18}O$ records from the Argentarola and Rio Martino caves in Italy and in Soreq Cave in Israel (Ayalon et al., 2002; Bard et al., 2002; Regattieri et al., 2021). It was interpreted as a period of higher rainfall and more ^{18}O depleted surface water in the Mediterranean region during deposition of sapropel S6.

The data presented in this study strongly support that the drop in sea surface $\delta^{18}O$ recorded in the Mediterranean at the onset of sapropel S6 and that centered at 150 ky can be at least partly attributed to the low $\delta^{18}O$ of the Atlantic inflow, as recorded at site 977 and PRGL1, although the prominent drop in the planktonic $\delta^{18}O$ in the Gulf of Lion and the Adriatic sea can be partially caused by meltwater released from the Alpine ice sheets through the Rhone and Po rivers that carry meltwater to the Gulf of Lion and the Adriatic sea, respectively. In consequence, the prominent $\delta^{18}O$ negative excursion seen in the Argentarola, Soreq and other speleothem records between 180 and 170 ky could be linked to the low $\delta^{18}O$ of the moisture originated in the Mediterranean basins at this time that carry the oxygen isotope imprint from Atlantic meltwater.

Based on these oxygen isotope records we argue that this meltwater from the Atlantic inflow and from the Alpine ice sheets played a key role on the final collapse of deep-water ventilation that resulted in the formation of sapropel S6. The onset of this sapropel precisely matches the onset of millennial warming event 6i of (Margari et al., 2010), suggesting that this abrupt increase in SST together with the previous meltwater input could have triggered the buoyancy gain interrupting deep water formation in the eastern Mediterranean. This correlation is corroborated by the abrupt warming and strong *Globigerinoides ruber* ^{18}O depletion recorded at the base of S6 in the eastern Mediterranean (Emeis et al., 2000; Casford et al., 2003; Kallel et al., 2000; Schmiedl et al., 2003; Thunell and Williams, 1983) that can be correlated with that recorded at site 977.

The impact of meltwater inflow starting at 178 ky does not exclude that freshwater from other sources could have played a role on the formation of sapropel S6 (Casford et al., 2003; Emeis et al., 2003; Kallel et al., 2000; Schmiedl et al., 2003; Thunell et al., 1983). An enhanced monsoon event observed at that time in Asian speleothems (Wang et al., 2008) or in the strong minimum of the Dole effect in Antarctic ice cores (Landais et al., 2010; Masson et al., 2000) could have further decrease the seawater $\delta^{18}O$ due to enhanced Nile discharge.

Bottom anoxia in S6 was less stable than in other sapropels (Casford et al., 2003; Schmiedl et al., 2003), suggesting that deep water formation in the Aegean and Adriatic seas was controlled by millennial changes of winter air temperature of the northerly winds that improved or prevent deep water formation. Two or three reoxygenation events were recorded in the middle of sapropel and only the lowermost part of the sapropel is completely devoid of benthic foraminifera (Casford et al., 2003; Schmiedl et al., 2003). This first phase of completely anoxic bottom waters is linked to the abrupt warming even 6i, while the reoxygenation events must be related to the abrupt cooling events occurring between 6i and 6iii.

The second meltwater period is registered between 157 and 145 ky in the sea surface δ^{18}O of the Atlantic inflow at site 977 (Fig. 7). Similar low planktic δ^{18}O values were also registered in the Gulf of Lion and in other sites of the Mediterranean during this time (Sierro et al., 2009) that could be partially linked to this meltwater inflow from the Atlantic. This last glacial maximum meltwater episode seems to have contributed too to reduce Mediterranean overturning as reflected by the low fine sand content and low benthic δ^{13}C values at site U1389 probably accompanied by other freshwater inputs from the Nile, etc. However, bottom water anoxia was never reached and no sapropel was deposited in the eastern Mediterranean, although an increase of the Ba/Al ratio at site ODP 968 (Ziegler et al., 2010) was probably the result of poor bottom water oxygenation that increased organic matter preservation, coinciding with the period of summer insolation maximum at circa 150 ky. A long gradual preconditioning phase depicted by the progressive decline of benthic δ^{13}C and decreasing fine sand seems to start with a brief event of poor ventilation during interstadial event 6v of (Margari et al., 2010), however, the minimum percentages of fine sand and minima in benthic δ^{13}C are not in phase. The lowermost fine sand contents, which we relate here with a weak MOW, occurred prior to the decrease in benthic δ^{13}C. We hypothesize that although both proxies indicate a weak MOW the later decrease of the benthic δ^{13}C may be influenced by the pronounced AMOC slowdown in the North Atlantic and the subsequent ^{13}C depletion in the north Atlantic intermediate waters during a time of reduced advection of the MOW. The remarkable event of meltwater from the European ice sheets recorded by large sediment discharge in the Bay of Biscay starting at around 160 ky (Boswel et al., 2019), which may be behind the freshwater input in the Mediterranean, also precedes the later slowdown of the AMOC at around 155 ky recorded by the decrease in benthic δ^{13}C in the north Atlantic (Barker et al., 2015). The coincidence of this drop in benthic δ^{13}C with widespread IRD (Ice Rafted Debris) deposition and cooling in the north Atlantic (Barker et al., 2015) clearly support this hypothesis.

It may be argued that this prominent Atlantic cooling and the cool northerly winds coming from continental Europe should have caused winter heat loss to the atmosphere in the northern seas of the Mediterranean (e.g. Gulf of Lion, Adriatic, Aegean seas) stimulating temperature driven convection and deep water ventilation that prevented sapropel formation, even though buoyancy gain associated to freshwater inputs was high.

10. Conclusions

A succession of abrupt, centennial to millennial climate changes, similar to the Dansgaard-Oeschger events recorded in the last glacial period, were recognized during the penultimate glacial period in the southwest Iberian margin, near the Strait of Gibraltar. They are similar to those recorded along the Portuguese margin but the higher sedimentation rate in the Gulf of Cadiz allowed the obtention of a climate record of much higher resolution for MIS6. The stadial/interstadial transitions are more regular and frequent during the period of ice sheet growth preceding the glacial maximum of MIS6. The number and frequency of the stadial-interstadial oscillations recorded in the *G. bulloides* δ^{18}O record is higher and more frequent than those previously observed in the SST records from the Iberian Margin during the penultimate glaciation.

While the planktic δ^{18}O record reflect climate changes in the Atlantic, the benthic δ^{18}O unambiguously revealed that this millennial variability had a strong impact on eastern Mediterranean climate that is the main source of the MOW at the Strait of Gibraltar. The benthic δ^{13}C and the content of fine sand in the sediments of site U1389 record past changes in the strength of the Mediterranean overflow after its exit through the Strait of Gibraltar. Abrupt changes in Mediterranean overturning circulation were recorded, with intense MOW during cool and dry events characterized by high benthic δ^{13}C and elevated sand content and slow MOW in warm and humid periods, characterized by low benthic δ^{13}C and sand content.

Two periods of special low MOW strengths were recorded by low benthic δ^{13}C and sand content during the penultimate glacial period that correspond to very weak overturning circulation in the Mediterranean during times of insolation maxima. The older one, centered at around 175 ky, was synchronous with the onset of "glacial sapropel" S6. A detailed correlation with the millennial events recorded in the Gulf of Cadiz indicates that the onset of this sapropel was triggered by the warming event 6i recorded in the Portuguese margin. A second period of weak overturning was centered at around 150 ky, but no sapropel was formed at that time. A new Monsoon chronology for MIS6 was elaborated based on the alignment of MOW weakening events at site U1389 with eastern Mediterranean sapropels and strong Asian monsoons. The comparison of this chronology with that of the atmospheric δ^{18}O from EDC in Antarctica (Extier et al., 2018) suggests that the AICC2012 time scale (Bazin et al., 2013) should be shifted to younger ages.

Seawater δ^{18}O records from site 977 at the entrance of the Mediterranean and PRGL1 in the Gulf of Lion provide evidence of the input of meltwater released from the ice sheets into the Mediterranean. This meltwater mainly delivered to the Atlantic, together with meltwater from the Alpine ice sheets, were important sources of freshwater that weakened the Mediterranean overturning during the formation of sapropel S6. The pronounced winter cooling caused by the meltwater released between 157 and 145 ky together with IRD probably prevented the formation of a sapropel in the eastern Mediterranean because of the great heat loss associated to the chilly winter northern winds in the northern seas of the Mediterranean that maintained high rates of deep water formation.

Credit author statement

Francisco J. Sierro: Writing the original draft, Writing -review and edition, Conceptualization, Investigation, Funding acquisition. **Nils Andersen:** Writing- review and editing, Conceptualization, Investigation, Validation.

Data availability

Data related to this article can be found at Mendeley Data https://doi.org/10.17632/ftm7dv42dp.1.

Declaration of competing interest

The authors declare that they have no known competing financial interests or personal relationships that could have appeared to influence the work reported in this paper.

Acknowledgements

The International Ocean Discovery Program is acknowledged for programming the expedition 339 to investigate the Mediterranean Outflow and providing the samples used in this study. We also appreciate the assistance of Jose Ignacio Martin Cruz for his invaluable work on sample processing and foraminifer picking. This work was funded by the Ministry of Economy of Spain Project RTI2018-099489-B-100 and Junta de Castilla y Leon UIC (Unidad de investigación consolidada) 102. Chronis Tzedakis and Vasiliki Margari are gratefully acknowledged for providing the pollen and benthic oxygen isotope data from core MD01-2444. Stephen Barker is acknowledged for providing the *N. pachyderma* left abundance data from ODP site 983.

References

Ambar, I., Howe, M.R., 1979. Observations of the Mediterranean outflow-I mixing in the Mediterranean outflow. Deep Sea Res. Part A, Oceanogr. Res. Pap. 26, 535–554. https://doi.org/10.1016/0198-0149(79)90095-5.

Ayalon, A., Bar-Matthews, M., Kaufman, A., 2002. Climatic conditions during marine oxygen isotope stage 6 in the eastern Mediterranean region from the isotopic composition of speleothems of Soreq Cave, Israel. Geology 30, 303–306. https://doi.org/10.1130/0091-7613(2002)030<0303:CCDMOI>2.0.CO, 2.

Badertscher, S., Fleitmann, D., Cheng, H., Edwards, R.L., Göktürk, O.M., Zumbühl, A., Leuenberger, M., Tüysüz, O., 2011. Pleistocene water intrusions from the mediterranean and caspian seas into the Black Sea. Nat. Geosci. 4, 236–239. https://doi.org/10.1038/ngeo1106.

Bahr, A., Kaboth, S., Jiménez-Espejo, F.J., Sierro, F.J., Voelker, A.H.L., Lourens, L., Röhl, U., Reichart, G.J., Escutia, C., Hernández-Molina, F.J., Pross, J., Friedrich, O., 2015. Persistent monsoonal forcing of mediterranean outflow water dynamics during the late Pleistocene. Geology 43. https://doi.org/10.1130/G37013.1.

Bard, E., Delaygue, G., Rostek, F., Antonioli, F., Silenzi, S., Schrag, D.P., 2002. Hydrological conditions over the western Mediterranean basin during the deposition of the cold Sapropel 6 (ca. 175 Kyr BP). Earth Planet Sci. Lett. 202, 481–494. https://doi.org/10.1016/S0012-821X(02)00788-4.

Barker, S., Chen, J., Gong, X., Jonkers, L., Knorr, G., Thornalley, D., 2015. Icebergs not the trigger for North Atlantic cold events. Nature 520, 333–336. https://doi.org/10.1038/nature14330.

Barker, S., Knorr, G., Conn, S., Lordsmith, S., Newman, D., Thornalley, D., 2019. Early interglacial legacy of deglacial climate instability. Paleoceanogr. Paleoclimatol. 34, 1455–1475. https://doi.org/10.1029/2019PA003661.

Barker, S., Knorr, G., Edwards, R.L., Parrenin, F., Putnam, A.E., Skinner, L.C., et al., 2011. 800,000 years of abrupt climate variability. Science 334 (6054), 347–351. https://doi.org/10.1126/science.1203580.

Batchelor, C.L., Margold, M., Krapp, M., Murton, D.K., Dalton, A.S., Gibbard, P.L., Stokes, C.R., Murton, J.B., Manica, A., 2019. The configuration of Northern Hemisphere ice sheets through the Quaternary. Nat. Commun. 10, 1–10. https://doi.org/10.1038/s41467-019-11601-2.

Bazin, L., Landais, A., Lemieux-Dudon, B., Toyé Mahamadou Kele, H., Veres, D., Parrenin, F., Martinerie, P., Ritz, C., Capron, E., Lipenkov, V., Loutre, M.-F., Raynaud, D., Vinther, B., Svensson, A., Rasmussen, S.O., Severi, M., Blunier, T., Leuenberger, M., Fischer, H., Masson-Delmotte, V., Chappellaz, J., Wolff, E., 2013. An optimized multi-proxy, multi-site Antarctic ice and gas orbital chronology (AICC2012): 120–800 ka. Clim. Past 9, 1715–1731. https://doi.org/10.5194/cp-9-1715-2013.

Bemis, B.E., Spero, H.J., Bijma, J., Lea, D.W., 1998. Reevaluation of the oxygen isotopic composition of planktonic foraminifera: experimental results and revised paleotemperature equations. Paleoceanography 13, 150–160. https://doi.org/10.1029/98PA00070.

Bintanja, R., Van de Wal, R.S.W., 2008. North American ice-sheet dynamics and the onset of 100,000-year glacial cycles. Nature 454, 869–872.

Bond, G., Broecker, W., Johnsen, S., McManus, J., Labeyrie, L., Jouzel, J., Bonani, G., 1993. Correlations between climate records from North Atlantic sediments and Greenland ice. Nature 365, 143–147. https://doi.org/10.1038/365143a0.

Bond, G.C., Lotti, R., 1995. Iceberg discharges into the north atlantic on millennial time scales during the last glaciation. Science 267, 1005–1010. https://doi.org/10.1126/science.267.5200.1005.

Boswel, S.M., Toucanne, S., Pitel-Roudaut, M., Creyts, T.T., Eynaud, F., Bayon, G., 2019. Enhanced surface melting of the fennoscandian ice sheet during periods of north Atlantic cooling. Geology 47, 664–668. https://doi.org/10.1130/g46370.1.

Broecker, W.S., 1998. Paleocean circulation during the Last Deglaciation: a bipolar seesaw? Paleoceanography 13, 119–121. https://doi.org/10.1029/97PA03707.

Cacho, I., Shackleton, N., Elderfield, H., Sierro, F.J., Grimalt, J.O., 2006. Glacial rapid variability in deep-water temperature and δ180 from the Western Mediterranean Sea. Quat. Sci. Rev. 25. https://doi.org/10.1016/j.quascirev.2006.10.004.

Casford, J.S.L., Rohling, E.J., Abu-Zied, R.H., Fontanier, C., Jorissen, F.J., Leng, M.J., Schmiedl, G., Thomson, J., 2003. A dynamic concept for eastern Mediterranean circulation and oxygenation during sapropel formation. Palaeogeogr. Palaeoclimatol. Palaeoecol. 190, 103–119. https://doi.org/10.1016/s0031-0182(02)00601-6.

Chappellaz, J., Brook, E., Blunier, T., Malaizé, B., 1997. CH_4 and $\delta^{18}O$ of O_2 records from Antarctic and Greenland ice: a clue for stratigraphic disturbance in the bottom part of the Greenland Ice Core Project and the Greenland Ice Sheet Project 2 ice cores. J. Geophys. Res. Ocean. 102, 26547–26557. https://doi.org/10.1029/97JC00164.

Cheng, H., Edwards, R.L., Sinha, A., Spotl, C., Yi, L., Chen, S.T., Kelly, M., Kathayat, G., Wang, X.F., Li, X.L., Kong, X.G., Wang, Y.J., Ning, Y.F., Zhang, H.W., 2016. The Asian monsoon over the past 640,000 years and ice age terminations. Nature 534, 640–646. https://doi.org/10.1038/nature20585.

Comas, M.C., Zahn, R., Klaus, A., et al., 1996. Proceedings of the Ocean Drilling Program, 161 Initial Reports, p. 161. https://doi.org/10.2973/odp.proc.ir.161.1996.

Cortina, A., Sierro, F.J., Flores, J.A., Martrat, B., Grimalt, J.O., 2015. The response of SST to insolation and ice sheet variability from MIS 3 to MIS 11 in the northwestern Mediterranean Sea (Gulf of Lions). Geophys. Res. Lett. 42 (10), 366–374. https://doi.org/10.1002/2015GL065539.

Cortina, A., Sierro, F.J., González-Mora, B., Asioli, A., Flores, J.A., 2011. Impact of climate and sea level changes on the ventilation of intermediate water and benthic foraminifer assemblages in the Gulf of Lions, off South France, during MIS 6 and 7. Palaeogeogr. Palaeoclimatol. Palaeoecol. 309, 215–228. https://doi.org/10.1016/j.palaeo.2011.06.005.

Dansgaard, W., Johnsen, S.J., Clausen, H.B., Dahl-Jensen, D., Gundestrup, N.S., Hammer, C.U., Hvidberg, C.S., Steffensen, J.P., Sveinbjörnsdottir, A.E., Jouzel, J., Bond, G., 1993. Evidence for general instability of past climate from a 250-kyr ice-core record. Nature 364, 218–220. https://doi.org/10.1038/364218a0.

de Abreu, L., Shackleton, N.J., Schonfeld, J., Hall, M., Chapman, M., 2003. Millennial-scale oceanic climate variability off the Western Iberian margin during the last two glacial periods. Mar. Geol. 196, 1–20. https://doi.org/10.1016/s0025-3227(03)00046-x.

de Castro, S., Hernández-Molina, F.J., de Weger, W., Jiménez-Espejo, F.J., Rodríguez-Tovar, F.J., Mena, A., Llave, E., Sierro, F.J., 2021. Contourite characterization and its discrimination from other deep-water deposits in the Gulf of Cadiz contourite depositional system. Sedimentology 68, 987–1027. https://doi.org/10.1111/sed.12813.

Emeis, K.-C., Schulz, H., Struck, U., Rossignol-Strick, M., Erlenkeuser, H., Howell, M.W., Kroon, D., Mackensen, A., Ishizuka, S., Oba, T., Sakamoto, T., Koizumi, I., 2003. Eastern Mediterranean surface water temperatures and $\delta^{18}O$ composition during deposition of sapropels in the late Quaternary. Paleoceanography 18. https://doi.org/10.1029/2000PA000617.

Emeis, K.C., Sakamoto, T., Wehausen, R., Brumsack, H.J., 2000. The sapropel record of the eastern mediterranean sea - results of ocean drilling Program leg 160. Palaeogeogr. Palaeoclimatol. Palaeoecol. 158, 371–395. https://doi.org/10.1016/s0031-0182(00)00059-6.

Extier, T., Landais, A., Bréant, C., Prié, F., Bazin, L., Dreyfus, G., Roche, D.M., Leuenberger, M., 2018. On the use of $\delta^{18}O_{atm}$ for ice core dating. Quat. Sci. Rev. 185, 244–257. https://doi.org/10.1016/j.quascirev.2018.02.008.

Eynaud, F., Zaragosi, S., Scourse, J.D., Mojtahid, M., Bourillet, J.F., Hall, I.R., Penaud, A., Locascio, M., Reijonen, A., 2007. Deglacial laminated facies on the NW European continental margin: the hydrographic significance of British-Irish Ice Sheet deglaciation and Fleuve Manche paleoriver discharges. G-cubed 8. https://doi.org/10.1029/2006gc001496.

Font, J., Millot, C., Salas, J., Julia, A., Chic, O., 1998. The drift of modified Atlantic water from the Alboran Sea to the eastern Mediterranean. Sci. Mar. 62, 211–216.

Goni, M.F.S., Landais, A., Fletcher, W.J., Naughton, F., Desprat, S., Duprat, J., 2008. Contrasting impacts of Dansgaard-Oeschger events over a western European latitudinal transect modulated by orbital parameters. Quat. Sci. Rev. 27, 1136–1151. https://doi.org/10.1016/j.quascirev.2008.03.003.

Goni, M.F.S., Turon, J.L., Eynaud, F., Gendreau, S., 2000. European climatic response to millennial-scale changes in the atmosphere-ocean system during the last glacial period. Quat. Res. 54, 394–403. https://doi.org/10.1006/qres.2000.2176.

Grant, K.M., Rohling, E.J., Ramsey, C.B., Cheng, H., Edwards, R.L., Florindo, F., Heslop, D., Marra, F., Roberts, A.P., Tamisiea, M.E., Williams, F., 2014. Sea-level variability over five glacial cycles. Nat. Commun. 5. https://doi.org/10.1038/ncomms6076.

Grimm, R., Maier-Reimer, E., Mikolajewicz, U., Schmiedl, G., Muller-Navarra, K., Adloff, F., Grant, K.M., Ziegler, M., Lourens, L.J., Emeis, K.C., 2015. Late glacial initiation of Holocene eastern Mediterranean sapropel formation. Nat. Commun. 6, 12. https://doi.org/10.1038/ncomms8099.

Hernandez-Molina, F.J., Sierro, F.J., Llave, E., Roque, C., Stow, D.A.V., Williams, T., Lofi, J., Van der Schee, M., Arnaiz, A., Ledesma, S., Rosales, C., Rodriguez-Tovari, F.J., Pardo-Iguzquiza, E., Brackenridge, R.E., 2016. Evolution of the gulf of Cadiz margin and southwest Portugal contourite depositional system: tectonic, sedimentary and paleoceanographic implications from IODP expedition 339. Mar. Geol. 377, 7–39. https://doi.org/10.1016/j.margeo.2015.09.013.

Hilgen, F.J., Lourens, L.J., Van Dam, J.A., Beu, A.G., Boyes, A.F., Cooper, R.A., Krijgsman, W., Ogg, J.G., Piller, W.E., Wilson, D.S., 2012. Chapter 29 - The Neogene Period. In: Gradstein, F.M., Ogg, J.G., Schmitz, M.D., Ogg, G.M. (Eds.), 810. Elsevier, Boston, pp. 923–978. https://doi.org/10.1016/B978-0-444-59425-9.00029-9.

Hodell, D., Crowhurst, S., Skinner, L., Tzedakis, P.C., Margari, V., Channell, J.E.T., Kamenov, G., Maclachlan, S., Rothwell, G., 2013a. Response of Iberian Margin sediments to orbital and suborbital forcing over the past 420 ka. Paleoceanography 28, 185–199.

Hodell, D.A., Lourens, L., Stow, D.A.V., Hernández-Molina, J., Alvarez Zarikian, C.A., Abrantes, F., Acton, G.D., Bahr, A., Balestra, B., Llave Barranco, E., Carrara, G., Crowhurst, S., Ducassou, E., Flood, R.D., Flores, J.-A., Furota, S., Grimalt, J., Grunert, P., Jimenez-Espejo, F.J., Kyoung Kim, J., Konijnendijk, T., Krissek, L.A., Kuroda, J., Li, B., Lofi, J., Margari, V., Martrat, B., Miller, M.D., Nanayama, F., Nishida, N., Richter, C., Rodrigues, T., Rodríguez-Tovar, F.J., Freixo Roque, A.C., Sanchez Goni, M.F., Sierro Sánchez, F.J., Singh, A.D., Skinner, L., Sloss, C.R., Takashimizu, Y., Tjallingii, R., Tzanova, A., Tzedakis, C., Voelker, A., Xuan, C., Williams, T., 2013b. The "Shackleton site" (IODP site U1385) on the iberian margin. Sci. Drill. 13–19. https://doi.org/10.5194/sd-16-13-2013.

Hughes, P.D., Woodward, J.C., Gibbard, P.L., 2006. Late pleistocene glaciers and climate in the mediterranean. Global Planet. Change 50, 83–98. https://doi.org/10.1016/j.gloplacha.2005.07.005.

Inge, J., Alexanderson, H., Astakhov, V.I., Demidov, I., Dowdeswell, A., Funder, S., Gataullin, V., Henriksen, M., Hjort, C., Houmark-nielsen, M., Hubberten, H.W., Jakobsson, M., Kjær, K.H., Larsen, E., Lokrantz, H., Pekka, J., Lys, A., Mangerud, J., Matiouchkov, A., Murray, A., Per, M., Niessen, F., Nikolskaya, O., Polyak, L., Saarnisto, M., Siegert, C., Siegert, M.J., Spielhagen, R.F., Stein, R., 2004. Late Quaternary ice sheet history of northern Eurasia 23, 1229–1271. https://doi.org/10.1016/j.quascirev.2003.12.008.

Johnsen, S.J., Clausen, H.B., Dansgaard, W., Fuhrer, K., Gundestrup, N., Hammer, C.U., Iversen, P., Jouzel, J., Stauffer, B., steffensen, J.P., 1992. Irregular glacial interstadials recorded in a new Greenland ice core. Nature 359, 311–313. https://doi.org/10.1038/359311a0.

Jouzel, J., Masson-Delmotte, V., Cattani, O., Dreyfus, G., Falourd, S., Hoffmann, G., Minster, B., Nouet, J., Barnola, J.M., Chappellaz, J., Fischer, H., Gallet, J.C., Johnsen, S., Leuenberger, M., Loulergue, L., Luethi, D., Oerter, H., Parrenin, F., Raisbeck, G., Raynaud, D., Schilt, A., Schwander, J., Selmo, E., Souchez, R., Spahni, R., Stauffer, B., Steffensen, J.P., Stenni, B., Stocker, T.F., Tison, J.L., Werner, M., Wolff, E.W., 2007. Orbital and millennial antarctic climate variability over the past 800,000 years. Science 317, 793–796. https://doi.org/10.1126/science.1141038.

Kaboth, S., Bahr, A., Reichart, G.J., Jacobs, B., Lourens, L.J., 2016. New insights into upper MOW variability over the last 150 kyr from IODP 339 Site U1386 in the Gulf of Cadiz. Mar. Geol. 377, 136–145. https://doi.org/10.1016/j.margeo.2015.08.014.

Kallel, N., Duplessy, J.C., Labeyrie, L., Fontugne, M., Paterne, M., Montacer, M., 2000. Mediterranean pluvial periods and sapropel formation over the last 200 000 years. Palaeogeogr. Palaeoclimatol. Palaeoecol. 157, 45–58. https://doi.org/10.1016/s0031-0182(99)00149-2.

Koltai, G., Sp, C., Otl, ∈, Shen, C.-C., Wu, C.-C., Rao, Z., Palcsu, L., Kele, S., Anyi, G.S., Ar Any-Kevei, I.B., 2017. A penultimate glacial climate record from southern Hungary. J. Quat. Sci. 32, 946–956. https://doi.org/10.1002/jqs.2968.

Konijnendijk, T.Y.M., Ziegler, M., Lourens, L.J., 2014. Chronological constraints on Pleistocene sapropel depositions from high-resolution geochemical records of ODP Sites 967 and 968. Newslett. Stratigr. 47, 263–282. https://doi.org/10.1127/0078-0421/2014/0047.

Landais, A., Dreyfus, G., Capron, E., Masson-Delmotte, V., Sanchez-Goñi, M.F., Desprat, S., Hoffmann, G., Jouzel, J., Leuenberger, M., Johnsen, S., 2010. What drives the millennial and orbital variations of δ18Oatm? Quat. Sci. Rev. 29, 235–246. https://doi.org/10.1016/j.quascirev.2009.07.005.

Laskar, J., Robutel, P., Joutel, F., Gastineau, M., Correia, A.C.M., Levrard, B., 2004. A long-term numerical solution for the insolation quantities of the Earth. Astron. Astrophys. 428, 261–285. https://doi.org/10.1051/0004-6361:20041335.

LeGrande, A.N., Schmidt, G.A., 2006. Global gridded data set of the oxygen isotopic composition in seawater. Geophys. Res. Lett. 33. https://doi.org/10.1029/2006GL026011.

Llave, E., Hernandez-Molina, F.J., Somoza, L., Diaz-del-Rio, V., Stow, D.A.V., Maestro, A., Dias, J.M.A., 2001. Seismic stacking pattern of the Faro-Albufeira contourite system (Gulf of Cadiz): a Quaternary record of paleoceanographic and tectonic influences. Mar. Geophys. Res. 22, 487–508. https://doi.org/10.1023/a:1016355801344.

Llave, E., Schonfeld, J., Hernandez-Molina, F.J., Mulder, T., Somoza, L., del Rio, V.D., Sanchez-Almazo, I., 2006. High-resolution stratigraphy of the Mediterranean outflow contourite system in the Gulf of Cadiz during the late Pleistocene: the impact of Heinrich events. Mar. Geol. 227, 241–262. https://doi.org/10.1016/j.margeo.2005.11.015.

Mangerud, J., Jakobsson, M., Alexanderson, H., Astakhov, V., Clarke, G.K.C., Henriksen, M., Hjort, C., Krinner, G., Lunkka, J.P., Moller, P., Murray, A., Nikolskaya, O., Saarnisto, M., Svendsen, J.I., 2004. Ice-dammed lakes and rerouting of the drainage of northern Eurasia during the Last Glaciation. Quat. Sci. Rev. 23, 1313–1332. https://doi.org/10.1016/j.quascirev.2003.12.009.

Margari, V., Skinner, L.C., Hodell, D.A., Martrat, B., Toucanne, S., Grimalt, J.O., Gibbard, P.L., Lunkka, J.P., Tzedakis, P.C., 2014. Land-ocean changes on orbital and millennial time scales and the penultimate glaciation. Geology 42, 183–186. https://doi.org/10.1130/g35070.1.

Margari, V., Skinner, L.C., Tzedakis, P.C., Ganopolski, A., Vautravers, M., Shackleton, N.J., 2010. The nature of millennial-scale climate variability during the past two glacial periods. Nat. Geosci. 3, 127–131. https://doi.org/10.1038/ngeo740.

Marino, G., Rohling, E.J., Rodriguez-Sanz, L., Grant, K.M., Heslop, D., Roberts, A.P., Stanford, J.D., Yu, J., 2015. Bipolar seesaw control on last interglacial sea level. Nature 522, 197–201. https://doi.org/10.1038/nature14499.

Martrat, B., Grimalt, J.O., Lopez-Martinez, C., Cacho, I., Sierro, F.J., Flores, J.A., Zahn, R., Canals, M., Curtis, J.H., Hodell, D.A., 2004. Abrupt temperature changes in the Western Mediterranean over the past 250,000 years. Science 306, 1762–1765. https://doi.org/10.1126/science.1101706.

Martrat, B., Grimalt, J.O., Shackleton, N.J., de Abreu, L., Hutterli, M.A., Stocker, T.F., 2007. Four climate cycles of recurring deep and surface water destabilizations on the Iberian margin. Science 317, 502–507.

Masson, V., Braconnot, P., Jouzel, J., De Nobler, N., Cheddadi, R., Marchal, O., 2000. Simulation of intense monsoons under glacial conditions. Geophys. Res. Lett. 27, 1747–1750. https://doi.org/10.1029/1999GL006070.

Mitsui, T., Crucifix, M., 2017. Influence of external forcings on abrupt millennial-scale climate changes: a statistical modelling study. Clim. Dynam. 48, 2729–2749. https://doi.org/10.1007/s00382-016-3235-z.

Nehme, C., Verheyden, S., Breitenbach, S.F.M., Gillikin, D.P., Verheyden, A., Cheng, H., Lawrence Edwards, R., Hellstrom, J., Noble, S.R., Farrant, A.R., Sahy, D., Goovaerts, T., Salem, G., Claeys, P., 2018. Climate dynamics during the penultimate glacial period recorded in a speleothem from Kanaan Cave, Lebanon (central Levant). Quat. Res. 90, 10–25. https://doi.org/10.1017/qua.2018.18.

Obrochta, S.P., Crowley, T.J., Channell, J.E.T., Hodell, D.A., Baker, P.A., Seki, A., Yokoyama, Y., 2014. Climate variability and ice-sheet dynamics during the last three glaciations. Earth Planet Sci. Lett. 406, 198–212. https://doi.org/10.1016/j.epsl.2014.09.004.

Peliz, A., Dubert, J., Santos, A.M.P., Oliveira, P.B., Le Cann, B., 2005. Winter upper ocean circulation in the western iberian basin - fronts, eddies and poleward flows: an overview. Deep. Res. Part I-Oceanographic Res. Pap. 52, 621–646. https://doi.org/10.1016/j.dsr.2004.11.005.

Peliz, A., Marchesiello, P., Santos, A.M.P., Dubert, J., Teles-Machado, A., Marta-Almeida, M., Le Cann, B., 2009. Surface circulation in the gulf of Cadiz: 2. Inflow-outflow coupling and the gulf of Cadiz slope current. J. Geophys. Res. 114. https://doi.org/10.1029/2008jc004771.

Penaud, A., Eynaud, F., Turon, J.L., Zaragosi, S., Malaizé, B., Toucanne, S., Bourillet, J.-F., 2009. What forced the collapse of European ice sheets during the last two glacial periods (150kaB. P. and 18ka cal BP)? Palynological evidence. Palaeogeogr. Palaeoclimatol. Palaeoecol. 281, 66–78.

Pickarski, N., Litt, T., 2017. A new high-resolution pollen sequence at Lake Van, Turkey: insights into penultimate interglacial-glacial climate change on vegetation history. Clim. Past 13, 689–710. https://doi.org/10.5194/cp-13-689-2017.

Pierre, C., 1999. The oxygen and carbon isotope distribution in the Mediterranean water masses. Mar. Geol. 153, 41–55. https://doi.org/10.1016/S0025-3227(98)00090-5.

Piva, A., Asioli, A., Andersen, N., Grimalt, J.O., Schneider, R.R., Trincardi, F., 2008. Climatic cycles as expressed in sediments of the PROMESS1 borehole PRAD1-2, central Adriatic, for the last 370 ka: 2. Paleoenvironmental evolution. GEOCHEMISTRY Geophys. GEOSYSTEMS 9. https://doi.org/10.1029/2007gc001785.

Regattieri, E., Querci, S., Zanchetta, G., Zanella, E., Isola, I., Drysdale, R.N., Hellstrom, J.C., Magrì, F., 2021. Interstadial conditions over the Southern Alps during the early penultimate glacial (MIS 6): a multiproxy record from Rio Martino Cave (Italy). Quat. Sci. Rev. 257, 106856. https://doi.org/10.1016/j.quascirev.2021.106856.

Rohling, E.J., Cane, T.R., Cooke, S., Sprovieri, M., Bouloubassi, I., Emeis, K.C., Schiebel, R., Kroon, D., Jorissen, F.J., Lorre, A., Kemp, A.E.S., 2002. African monsoon variability during the previous interglacial maximum. Earth Planet Sci. Lett. 202, 61–75. https://doi.org/10.1016/s0012-821x(02)00775-6.

Rohling, E.J., Marino, G., Grant, K.M., 2015. Mediterranean climate and oceanography, and the periodic development of anoxic events (sapropels). Earth Sci. Rev. 143, 62–97. https://doi.org/10.1016/j.earscirev.2015.01.008.

Rossignol-Strick, M., 1983. African monsoons, an immediate climate response to orbital insolation. Nature 304, 46–49. https://doi.org/10.1038/304046a0.

Roucoux, K.H., Tzedakis, P.C., Lawson, I.T., Margari, V., 2011. Vegetation history of the penultimate glacial period (Marine Isotope Stage 6) at Ioannina, north-west Greece. J. Quat. Sci. 26, 616–626. https://doi.org/10.1002/jqs.1483.

Sanchez-Leal, R.F., Bellanco, M.J., Fernandez-Salas, L.M., Garcia-Lafuente, J., Gasser-Rubinat, M., Gonzalez-Pola, C., Hernandez-Molina, F.J., Pelegri, J.L., Peliz, A., Relvas, P., Roque, D., Ruiz-Villarreal, M., Sammartino, S., Sanchez-Garrido, J.C., 2017. The mediterranean overflow in the gulf of Cadiz: a rugged journey. Sci. Adv. 3. https://doi.org/10.1126/sciadv.aao0609 eaao0609–eaao0609.

Schmiedl, G., Mitschele, A., Beck, S., Emeis, K.C., Hemleben, C., Schulz, H., Sperling, M., Weldeab, S., 2003. Benthic foraminiferal record of ecosystem variability in the eastern Mediterranean Sea during times of sapropel S5 and S6 deposition. Palaeogeogr. Palaeoclimatol. Palaeoecol. 190, 139–164. https://doi.org/10.1016/S0031-0182(02)00603-X.

Shackleton, N.J., Hall, M.A., Vincent, E., 2000. Phase relationships between millennial-scale events 64,000-24,000 years ago. Paleoceanography 15, 565–569. https://doi.org/10.1029/2000pa000513.

Shin, J., Nehrbass-Ahles, C., Grilli, R., Chowdhry Beeman, J., Parrenin, F., Teste, G., Landais, A., Schmidely, L., Silva, L., Schmitt, J., Bereiter, B., Stocker, T.F., Fischer, H., Chappellaz, J., 2020. Millennial-scale atmospheric CO_2 variations during the marine isotope stage 6 period (190-135ka). Clim. Past 16, 2203–2219. https://doi.org/10.5194/cp-16-2203-2020.

Sierro, F.J., Andersen, N., Bassetti, M.A., Berné, S., Canals, M., Curtis, J.H., Dennielou, B., Flores, J.A., Frigola, J., Gonzalez-Mora, B., Grimalt, J.O., Hodell, D.A., Jouet, G., Pérez-Folgado, M., Schneider, R., 2009. Phase relationship between sea level and abrupt climate change. Quat. Sci. Rev. 28, 2867–2881. https://doi.org/10.1016/j.quascirev.2009.07.019.

Sierro, F.J., Flores, J.A., Baraza, J., 1999. Late glacial to recent paleoenvironmental changes in the Gulf of Cadiz and formation of sandy contourite layers. Mar. Geol. 155, 157–172. https://doi.org/10.1016/S0025-3227(98)00145-5.

Sierro, F.J., Hodell, D.A., Andersen, N., Azibeiro, L.A., Jimenez-Espejo, F.J., Bahr, A.,

Flores, J.A., Ausin, B., Rogerson, M., Lozano-Luz, R., Lebreiro, S.M., Hernandez-Molina, F.J., 2020. Mediterranean overflow over the Last 250 Kyr: Freshwater Forcing from the Tropics to the Ice Sheets. Paleoceanogr. Paleoclimatol. 35. https://doi.org/10.1029/2020PA003931.
Skinner, L.C., Elderfield, H., 2007. Rapid fluctuations in the deep North Atlantic heat budget during the last glacial period. Paleoceanography 22, 9. https://doi.org/10.1029/2006pa001338.
Skinner, L.C., Shackleton, N.J., Elderfield, H., 2003. Millennial-scale variability of deep-water temperature and delta O-18(dw) indicating deep-water source variations in the Northeast Atlantic, 0-34 cal. ka BP. G-cubed 4. https://doi.org/10.1029/2003gc000585.
Soto-Navarro, J., Criado-Aldeanueva, F., Sanchez-Garrido, J.C., Garcia-Lafuente, J., 2012. Recent thermohaline trends of the Atlantic waters inflowing to the Mediterranean Sea. Geophys. Res. Lett. 39, 7. https://doi.org/10.1029/2011gl049907.
Stocker, T.F., 1998. The seesaw effect. Science 282, 61. https://doi.org/10.1126/science.282.5386.61. LP − 62.
Stow, D.A.V., Hernández-Molina, F.J., Alvarez Zarikian, C.A., 2013a. Proceedings of the IODP, 339. Expedition 339 Scientists. Integrated Ocean Drilling Program Management International, Inc., Tokyo https://doi.org/10.2204/iodp.proc.339.2013.
Stow, D.A.V., Hernandez-Molina, F.J., Llave, E., Bruno, M., Garcia, M., del Rio, V.D., Somoza, L., Brackenridge, R.E., 2013b. The Cadiz Contourite Channel: sandy contourites, bedforms and dynamic current interaction. Mar. Geol. 343, 99−114. https://doi.org/10.1016/j.margeo.2013.06.013.
Thunell, R.C., Williams, D.F., 1983. Paleotemperature and paleosalinity history of the estern mediterranean during the late quaternary. Palaeogeogr. Palaeoclimatol. Palaeoecol. 44, 23−39. https://doi.org/10.1016/0031-0182(83)90003-2.
Thunell, R.C., Williams, D.F., Cita, M.B., 1983. Glacial anoxia in the eastern Mediterranean. J. Foraminifer. Res. 13, 283−290. https://doi.org/10.2113/gsjfr.13.4.283.
Toucanne, S., Mulder, T., Schonfeld, J., Hanquiez, V., Gonthier, E., Duprat, J., Cremer, M., Zaragosi, S., 2007. Contourites of the Gulf of Cadiz: a high-resolution record of the paleocirculation of the Mediterranean outflow water during the last 50,000 years. Palaeogeogr. Palaeoclimatol. Palaeoecol. 246, 354−366. https://doi.org/10.1016/j.palaeo.2006.10.007.
Toucanne, S., Zaragosi, S., Bourillet, J.-F., Cremer, M., Eynaud, F., Van Vliet-Lanoë, B., Penaud, A., Fontanier, C., Turon, J.L., Cortijo, E., 2009. Timing of massive 'Fleuve Manche'discharges over the last 350kyr: insights into the European ice-sheet oscillations and the European drainage network from MIS 10 to 2. Quat. Sci. Rev. 28, 1238−1256.
Troelstra, S.R., Ganssen, G.M., van der Borg, K., de Jong, A.F.M., 1991. A late quaternary stratigraphic framework for eastern mediterranean sapropel S1 based on AMS 14C dates and stable oxygen isotopes. Radiocarbon 33, 15−21. https://doi.org/10.1017/S0033822200013175.
Tzedakis, P.C., Crucifix, M., Mitsui, T., Wolff, E.W., 2017. A simple rule to determine which insolation cycles lead to interglacials. Nature 542, 427−432. https://doi.org/10.1038/nature21364.
Tzedakis, P.C., Drysdale, R.N., Margari, V., Skinner, L.C., Menviel, L., Rhodes, R.H., Taschetto, A.S., Hodell, D.A., Crowhurst, S.J., Hellstrom, J.C., Fallick, A.E., Grimalt, J.O., McManus, J.F., Martrat, B., Mokeddem, Z., Parrenin, F., Regattieri, E., Roe, K., Zanchetta, G., 2018. Enhanced climate instability in the north atlantic and southern Europe during the last interglacial. Nat. Commun. 9, 4235. https://doi.org/10.1038/s41467-018-06683-3.
Veres, D., Bazin, L., Landais, A., Toyé Mahamadou Kele, H., Lemieux-Dudon, B., Parrenin, F., Martinerie, P., Blayo, E., Blunier, T., Capron, E., Chappellaz, J., Rasmussen, S.O., Severi, M., Svensson, A., Vinther, B., Wolff, E.W., 2013. The Antarctic ice core chronology (AICC2012): an optimized multi-parameter and multi-site dating approach for the last 120 thousand years. Clim. Past 9, 1733−1748. https://doi.org/10.5194/cp-9-1733-2013.
Voelker, A.H.L., Colman, A., Olack, G., Waniek, J.J., Hodell, D., 2015. Oxygen and hydrogen isotope signatures of Northeast Atlantic water masses. Deep Sea Res. Part II Top. Stud. Oceanogr. 116, 89−106.
Voelker, A.H.L., de Abreu, L., 2011. A review of abrupt climate change events in the northeastern atlantic ocean (iberian margin): latitudinal, longitudinal, and vertical gradients. In: Rashid, H., Polyak, L., MosleyThompson, E. (Eds.), Abrupt Climate Change: Mechanisms, Patterns, and Impacts. Amer Geophysical Union, Washington, pp. 15−37. https://doi.org/10.1029/2010gm001021.
Voelker, A.H.L., Lebreiro, S.M., Schonfeld, J., Cacho, I., Erlenkeuser, H., Abrantes, F., 2006. Mediterranean outflow strengthening during northern hemisphere coolings: a salt source for the glacial Atlantic? Earth Planet Sci. Lett. 245, 39−55. https://doi.org/10.1016/j.epsl.2006.03.014.
Wainer, K., Genty, D., Blamart, D., Bar-Matthews, M., Quinif, Y., Plagnes, V., 2013. Millennial climatic instability during penultimate glacial period recorded in a south-western France speleothem. Palaeogeogr. Palaeoclimatol. Palaeoecol. 376, 122−131. https://doi.org/10.1016/j.palaeo.2013.02.026.
Wainer, K., Genty, D., Blamart, D., Daeron, M., Bar-Matthews, M., Vonhof, H., Dublyansky, Y., Pons-Branchu, E., Thomas, L., van Calsteren, P., Quinif, Y., Caillon, N., 2011. Speleothem record of the last 180 ka in Villars cave (SW France): Investigation of a large delta O-18 shift between MIS6 and MIS5. Quat. Sci. Rev. 30, 130−146. https://doi.org/10.1016/j.quascirev.2010.07.004.
Wang, Y., Cheng, H., Edwards, R.L., Kong, X., Shao, X., Chen, S., Wu, J., Jiang, X., Wang, X., An, Z., 2008. Millennial- and orbital-scale changes in the East Asian monsoon over the past 224,000 years. Nature 451, 1090−1093. https://doi.org/10.1038/nature06692.
Wegwerth, A., Dellwig, O., Kaiser, J., Menot, G., Bard, E., Shumilovskikh, L., Schnetger, B., Kleinhanns, I.C., Wille, M., Arz, H.W., 2014. Meltwater events and the mediterranean reconnection at the saalian-eemian transition in the Black Sea. Earth Planet Sci. Lett. 404, 124−135. https://doi.org/10.1016/j.epsl.2014.07.030.
Wegwerth, A., Kaiser, J., Dellwig, O., Arz, H.W., 2020. Impact of eurasian ice sheet and north Atlantic climate dynamics on Black Sea temperature variability during the penultimate glacial (MIS 6, 130−184 ka BP). Paleoceanogr. Paleoclimatol. 35. https://doi.org/10.1029/2020PA003882.
Wilson, G.P., Frogley, M.R., Hughes, P.D., Roucoux, K.H., Margari, V., Jones, T.D., Leng, M.J., Tzedakis, P.C., 2021. Persistent millennial-scale climate variability in southern Europe during marine isotope stage 6. Quat. Sci. Adv. 3, 100016. https://doi.org/10.1016/j.qsa.2020.100016.
Ziegler, M., Tuenter, E., Lourens, L.J., 2010. The precession phase of the boreal summer monsoon as viewed from the eastern Mediterranean (ODP Site 968). Quat. Sci. Rev. 29, 1481−1490. https://doi.org/10.1016/j.quascirev.2010.03.011.